HIV corruption of the Arp2/3-Cdc42-IQGAP1 axis to hijack cortical F-Actin to promote cell-cell viral spread.

Anupriya Aggarwal[1], Alberto Ospina Stella[1], Catherine Henry[2,3,*] , Kedar Narayan[2,3] & Stuart G. Turville[1]

[1] The Kirby Institute, University of New South Wales, New South Wales, Australia.
[2] Center for Molecular Microscopy, Center for Cancer Research, National Cancer Institute, National Institutes of Health, Bethesda, Maryland, USA.
[3] Cancer Research Technology Program, Frederick National Laboratory for Cancer Research, Frederick, Maryland, USA.
[*] Current address: David H. Koch Institute for Integrative Cancer Research, Massachusetts Institute of Technology, Cambridge, MA, United States

Corresponding Author:
Stuart G. Turville
The Kirby Institute, UNSW Australia
Office 529 Level 5 Wallace Wurth Building,
UNSW, Sydney NSW 2052
Telephone: +61 (02) 9385 0462
Email: sturville@kirby.unsw.edu.au

Abstract

F-Actin remodelling is important for the spread of HIV via cell-cell contacts, yet the mechanisms by which HIV corrupts the actin cytoskeleton are poorly understood. Through live cell imaging and focused ion beam scanning electron microscopy (FIB-SEM), we observed F-Actin structures that exhibit strong positive curvature to be enriched for HIV buds. Virion proteomics, gene silencing, and viral mutagenesis supported a Cdc42-IQGAP1-Arp2/3 pathway as the primary intersection of HIV budding, membrane curvature and F-Actin regulation. Whilst HIV egress activated the Cdc42-Arp2/3 filopodial pathway, this came at the expense of cell-free viral release. Importantly, release could be rescued by cell-cell contact, provided Cdc42 and IQGAP1 were present. From these observations we conclude that out-going HIV has corrupted a central F-Actin node that enables initial coupling of HIV buds to cortical F-Actin to place HIV at the leading cell edge. Whilst this initially prevents particle release, maturation of cell-cell contacts signals back to this F-Actin node to enable viral release & subsequent infection of the contacting cell.

Introduction

Actin is a major component of the cellular cytoskeleton and is present in both monomeric globular (G-actin) and polymeric filamentous (F-actin) forms in all eukaryotic cells. Specifically in human leukocytes, actin accounts for over 10% of the total protein content [1] and is a prerequisite for many pathways involved in communication of the immune response, such as chemotaxis of leukocytes through to the formation of supramolecular structures like the immunological synapse- a fundamental structure driving the primary immune response [2,3]. While cells encode a wide range of proteins that mediate F-actin remodelling, the critical ability to seed or 'nucleate' F-actin from the monomeric G-actin pool is limited to only a few protein families [4]. The two major classes of cellular actin nucleators are the Arp2/3 complex and formins [5]. The Arp2/3 complex is composed of 7 different subunits and allows formation of branched actin networks, through nucleation of a branch filament from an existing mother filament at an angle of 70 degrees [6,7]. In contrast, formins are large multidomain proteins that drive nucleation and/or elongation of unbranched linear actin filaments (reviewed in [4,8]. The activity of cellular Arp2/3 and formins is tightly regulated by a complex network of signalling pathways that primarily rely on the molecular switch properties of Rho-GTPases, such as Rac1 and Cdc42, for their activation [9,10].

HIV infection and spread proceeds primarily in CD4 positive leukocytes of our immune system [11]. Viral spread can be observed at two levels. Firstly, free virus release from infected cells, with virions travelling in a cell-free form until encountering a new target cell to infect. Secondly, HIV budding that occurs directly at sites of cell-cell contact. The supramolecular structure that enables the latter and highly efficient cell-cell viral transfer is referred to as the virological synapse (VS) [12,13]. In both cases, viral budding needs to proceed at the plasma membrane (PM) of infected cells and is initially driven by oligomerisation of the HIV structural protein Gag [14] and culminates with HIV particle abscission mediated by cellular proteins of the endosomal sorting complexes required for transport machinery (ESCRT) [15]. Several F-actin structures have been previously observed in association with HIV assembly and higher-level Gag oligormerisation. These include; the temporal formation of F-Actin asters/stars that appear just underneath the PM prior to particle release [16], and assembling HIV particles decorating the tips of finger-like filopodial structures [17-19]. It is however unclear how these events are mechanistically connected and how coupling to the F-actin cytoskeleton benefits HIV release/spread [20]. This can be considered at two-levels: firstly how does F-Actin regulation influence the assembly and release of cell free virus in infected cells? For instance, do cortical F-Actin structures facilitate HIV assembly and release at the PM as observed for other viruses [21]? Secondly, how is F-actin regulated at cell-cell contacts involving HIV infected cells? Several studies have shown that functional actin dynamics are required for cell-cell viral transfer [13,22], yet how HIV assembly and release are spatiotemporally coordinated during this process has not been clarified mechanistically.

With our primary aim to determine the role for F-Actin in cell-free HIV egress and cell-cell viral transfer, herein we peeled back the complexity of F-Actin regulation in leukocytes by successive depletion and/or knockout of key actin nucleators and other associated proteins that regulate their activity. In doing so, we biased the formation of different cortical F-Actin structures such as filopodia and lamellipodia. Herein we define these structures as outlined by Mattila and Lappalain, i.e. Filopodia are cylindrical finger like protrusions approximately 100–300 nm in diameter and up to 1μm to 10 μm or more in length, whereas lamellipodia are thin (100 nm to 200 nm thick) sheet/viel like cortical F-Actin protusions [23]. Whilst the regulation of lamellipodia is well understood and primarily depends on branched F-actin nucleation by

the Arp2/3 complex downstream of Rac1 and its effector Wave2 [24-29], various models have been proposed for filopodia formation and increasing evidence suggests this process may be cell-type specific [23,30]. Importantly, little is known about the mechanism of filopodia formation in cells of hematopoietic lineage, despite the fact that filopodia play important roles in immune cell function.

Using a combination of live cell imaging, focused ion beam scanning electron microscopy (FIB-SEM), virion mass spectrometry and viral infection assays, we observed the influence of HIV on cortical F-Actin at several levels. First, FIB-SEM revealed HIV budding to be relatively enriched in areas of high positive membrane curvature within Arp2/3-dependent cortical F-Actin structures, including filopodia and lamellipodia. Second, virion mass spectrometry identified a cortical F-Actin signalling node comprising of the Arp2/3 related GTPases Rac1 and Cdc42 and their binding partner, the scaffolding protein IQGAP1. Finally, while depletion of a number of dominant F-actin regulators was observed to affect free virus release, cell-cell viral transfer was only significantly impaired in cells depleted of Cdc42 or IQGAP1. Collectively these observations support a dominant role of the GTPase Cdc42 and IQGAP1 in the final stages of viral egress and cell-cell spread. In this setting we propose HIV manipulation of the Cdc42/IQGAP1 node to be important at two levels: firstly it enables HIV to be embedded and retained in Arp2/3-dependent leading edge structures that are important during pre-synaptic events. Secondly, as the VS is engaged and matures, the same regulators likely coordinate F-Actin dynamics to enable conditions that facilitate final viral particle release.

Results

Moulding cortical F-Actin through formin and Arp2/3 depletion

A physical association of HIV with F-actin structures has been previously observed in all major HIV primary target cell types [18,31]. In infected CD4+ T-cells and dendritic cells this manifests in the form of HIV-Filopodia, which are F-actin rich finger-like structures with HIV assembly observed at their tips [18]. Since these structures are more prominent on dendritic cells and similarly enriched in U937 cells [18,32,33], this latter myeloid cell line provides an ideal model to dissect the link between F-Actin and HIV assembly in the specific context of hematopoietic cell lineages. Given the proposed role of Arp2/3 and formins in filopodia formation in other cell types, we initially focused on these key actin regulators for depletion. However, while Arp2/3 is ubiquitously expressed in eukaryotic cells, there are at least 15 different formins in vertebrates [34,35]. Since Diaph1, Diaph2 and FMNL1 are the most abundantly expressed in leukocytes [36], we tailored our initial shRNA screening to depletion of these formins. Disruption of filopodial networks was assessed by measuring filopodial abundance (average number of filopodia per cell) and length (average filopodial length measured from the PM to the tip). To this end we used several imaging techniques at increasing levels of resolution, including; i) live cell imaging, ii) fixed cell fluorescence imaging followed by 3D deconvolution, and iii) the power of correlative FIB-SEM to finely resolve F-Actin structures closer to the PM. In brief, FIB-SEM represents a method where iterative cycles of finely tuned ion abrasion milling are followed by high-resolution scanning electron microscopy of heavy-metal stained, resin-embedded cell samples [37,38]. The end result is the recording of a stack of 2D back-scatter electron images, which are then processed and converted to a 3D image volume, typically at ~ 10 nm pixel sampling (Fig.1 B-E). This method provides a powerful imaging tool for cell biology and virology, as it gives users the ability to resolve nanoscale

ultrastructural features in cellular samples that may appear in association with viral particles [39,40].

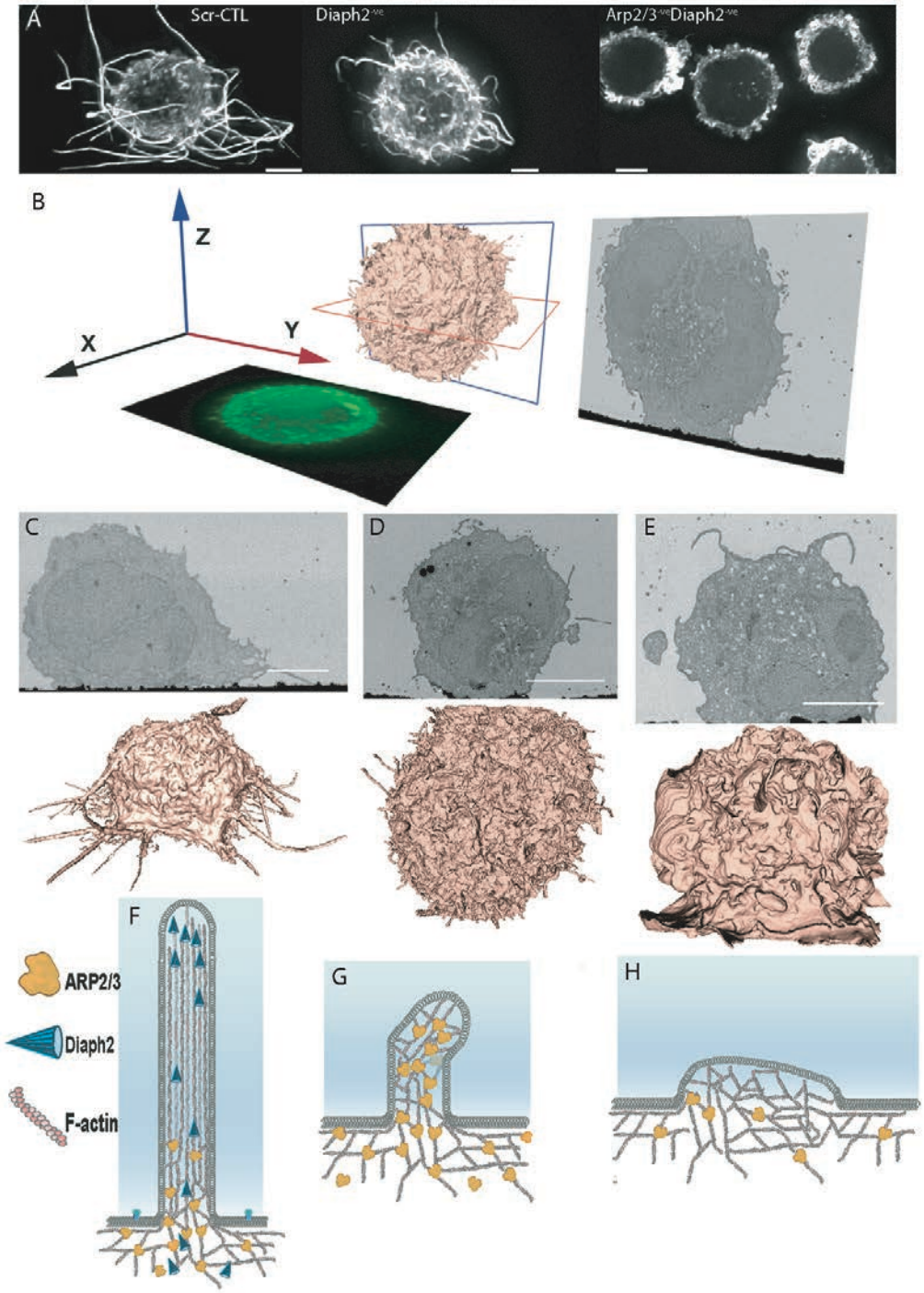

Figure 1. Depletion of F-actin regulators reveals long filopodial networks to be driven by Arp2/3 and Diaph2.

A. F-Actin staining by phalloidin Alexa-647 reveals extensive and long filopodia in uninfected scramble shRNA control cells (Scr-CTL), short abundant filopodia upon deletion of the formin Diaph2, and extensive lamellipodia when both Diaph2 and Arp2/3 are co-depleted. B. Schematic representation of FIB-SEM imaging data. C-E. FIB-SEM 2D images (upper) and 3D reconstructions (lower) of C. non-depleted control cells (Scr-CTL), D. Diaph2-depleted cells and E. Diaph2 and Arp2/3 co-depleted cells. All scale bars are 5µm. F-H. Schematic

representation of phenotypes induced by loss of F-Actin regulators. F. Wildtype scenario, G. Diaph2 deficiency, H. Diaph2 & Arp2/3deficiency. Note in H. we represent reduced levels of Arp2/3, given its high cellular abundance and residual levels of Arp2/3 in our knockdown cells (Fig. S3).

Initial experiments revealed filopodial lengths to be dependent solely on the formin Diaph2 and not the other leukocyte-enriched formins (Fig. S1). Silencing of Diaph2 by shRNA achieved >95% depletion at the protein level (Fig. S3), and in these cells cortical F-Actin coalesced into a network of abundant and short (1 to 3µm) filopodia (Fig. 1E&H; Movie S1). Since we could confirm this phenotype in CRISPR/Cas9-generated and clonally expanded Diaph2 homozygous knockout cells, our observations suggest that filopodial length but not seeding is dependent on Diaph2. Subsequent shRNA codepletion of other expressed formins in addition to Diaph2 did also not disrupt this short filopodial network (Fig. S1). Therefore, to test if the shorter but more abundant filopodia were Arp2/3-dependent, we disrupted both Diaph2 and the Arp2/3 complex by shRNA. Co-depletion led to short filopodia converging into an extensive lamellipodial network (Fig. 1A,E&H; Movie S2). To conclude, we could readily control cortical F-Actin within this leukocyte landscape, and generate three unique cell types with a continuum of cortical F-actin structures; i) long filopodia, ii) abundant short filopodia, and iii) an extensive network of large lamellipodia. Furthermore, our observations indicate that seeding of filopodia in myeloid cells requires Arp2/3-mediated actin nucleation, whereas filopodial elongation is dependent on the formin Diaph2 (Fig. 1. F-H).

<u>The influence of shifting F-Actin structures on the location of HIV budding</u>

In the context of HIV infected cells, we used our high-resolution imaging approaches to probe for a possible link between HIV assembly and specific F-Actin structures and/or pathways in leukocytes. Previously we have observed live cells with long filopodia to have significant numbers of HIV positive tips [18], and readily concluded that in untreated cells HIV assembly is enriched to this site. However, detection of HIV buds in cells with short filopodia (i.e. depleted of Diaph2) was constrained by the inability to resolve F-Actin structures proximal to the PM by fluoresecence microscopy alone. Thus, we applied FIB-SEM imaging to HIV-infected Diaph2^{-ve} cells (short filopodia) and observed HIV buds in routine association with the tip and sides of these structures (Fig. 2A,B,E&H). In cells with prominent lamellipodia (Diaph2^{-ve}Arp2/3^{-ve}), FIB-SEM imaging revealed abundance of HIV buds along the ridges of lamellipodia (Fig. 2F&K; Movie S2). Therefore one common feature of each F-Actin structure was the appearance of HIV preferentially in areas of positive membrane curvature. Given the large topological differences between filopodia and lamellipodia, we assessed viral-bud density by accounting for the surface area available for budding within each distinct F-Actin structure. This revealed HIV buds to be significantly enriched in areas of high positive membrane curvature (Table SI; Fig. 2 G-L): Lamellipodial ridges and filopodia were the most active areas of viral assembly, with a distinct preference for the latter (filopodia tips outscored lamellipodial ridges by 5-fold, when surface area was considered). This observation supports two potential mechanisms. First, HIV assembly is facilitated by areas of positive curvature or alternatively, HIV assembly recruits/influences cellular protein(s) at the PM that can lead to positive curvature.

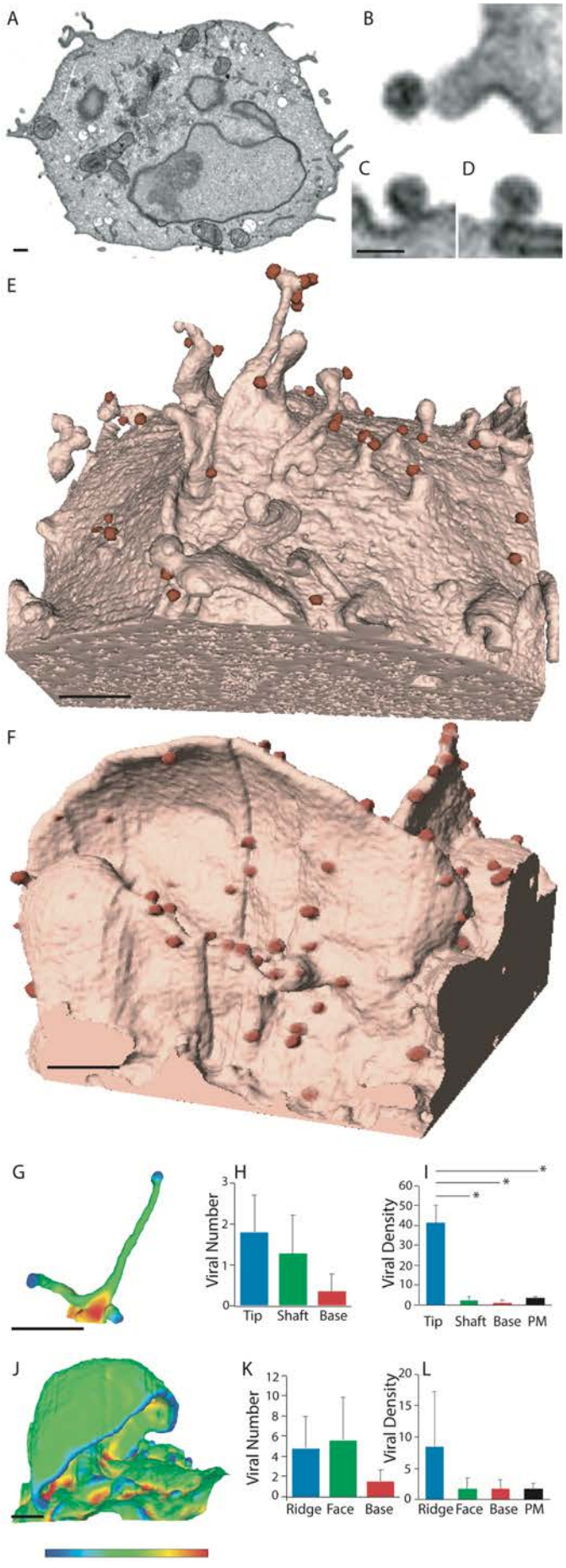

Figure 2. HIV budding enriched to positively curved cortical F-Actin.

A-D Representative FIB-SEM images of HIV virions associated with B. Filopodia and C-D plasma membrane of a HIV infected cell depleted of Diaph2. E.-F. 3D rendering FIB-SEM images of HIV infected E. Diaph2^{-ve} and F. Diaph2^{-ve}Arp2/3^{-ve} cell clones. HIV buds are shaded in red to highlight their location. G&J. enumeration of HIV-buds in association with positively curved cortical F-Actin structures. G. Filopodia and J. lamellipodia are pseudocolored using a colour spectrum from blue (positive curvature), green (neutral curvature) to red (negative curvature). H-I Enumeration of total HIV buds in association with the filopodia in Diaph2^{-ve} cells. H. Absolute viral bud counts and I. HIV bud density per µm^2. K-L. Enumeration of total HIV buds in association with the lamellipodia in Diaph2^{-ve} Arp2/3^{-ve} cells. K. Absolute viral bud counts and L. HIV bud density per µm^2. All scale bars are 0.5µm with the exception of B-D, which is 0.1µm. Bar graphs in H-I represent mean and standard deviations of virion counts from n = 15 filopodial structures. K-L bar graphs represent mean and standard deviations of virion counts from n = 15 lamellipodial structures. Statistics for panels G-L are summarised in Table SI. *P>0.05

Filopodia dominated by the formin Diaph2 present positive curvature at the plasma membrane but exclude assembling HIV particles

To assess whether strong positive membrane curvature alone was sufficient to position HIV buds at filopodial tips, we induced long filopodia using a constitutively active (C/A) mutant of Diaph2. Diaphanous-related formins exist in an autoinhibited conformation mediated by the interaction between their N-proximal inhibitory domain (DID) and C-terminal autoregulatory domain (DAD) [36,41]. Disruption of this autoinhibitory state can be achieved by formins binding to Rho-GTPases or, as in our case, by deletion of their C-terminal DAD domain [42,43]. Importantly, in both cases the central actin polymerization domain of the formin is rendered constitutively active.

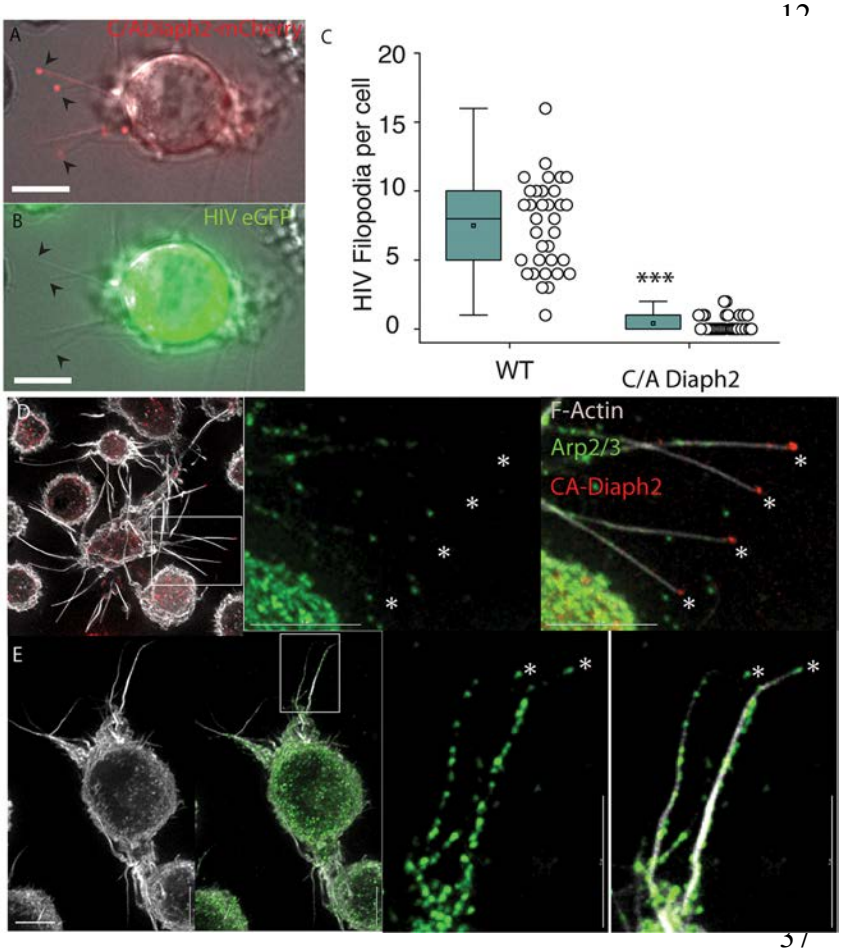

Figure 3. Constitutively active Diaph2 driven Filopodia are not associated with HIV buds. A & B. Live still images from supplement Movie S3; A. $^{C/A}$Diaph2-mCherry (red) positive cells, infected with B. HIViGFP (green). Note Diaph2 at the tips of filopodia are negative for HIV. Scale bars are at 5µm. C. Quantification of HIV postive filopodia per cell in HIV infected live cell cultures. HIV filopodia counts pooled from three independent HIV infections ***p<0.0001. D&E. Immunofluorescent Arp2/3 staining of D. $^{C/A}$Diaph2-mCherry (red) positive cells and E. Untreated cells. Asterisks highlight the terminal ends of filopodia that are either Diaph2 positive & Arp2/3 negative (for $^{C/A}$Diaph2-mCherry) or Arp2/3 positive (for untreated cells).

If HIV assembly was directly promoted by positive membrane curvature, filopodia induced by Diaph2$^{C/A}$ would incorporate assembling viral particles. However, while Diaph2$^{C/A}$ expression readily induced the formation of long straight filopodia with Diaph2 accumulating at the filopodial tips (Fig. 3A & Movie S3), in HIV infected cells we also observed complete exclusion of HIV particles from the tips of these structures (Fig. 3A-C & Movie S3). Therefore, the strong membrane curvature in filopodial tips alone is not sufficient to recruit HIV assembly to this region. Since long filopodia in WT cells are routinely HIV positive, whereas straight C/A Diaph2 driven filopodia are not, it is unlikely that formins represent the link of HIV to the F-actin cytoskeleton. We then turned our attention to the Arp2/3 complex, given that previous observations propose this as the dominant F-actin nucleator at the cell cortex, with formin activity being restricted to filament elongation post F-actin nucleation [44,45]. To confirm if Arp2/3 was the dominant filopodial nucleator in WT versus Diaph2$^{C/A}$ cells, we immunostained filopodia for Arp2/3, and examined the footprint of this nucleator along the filopodial body and tip. In both cell types, the filopodial bases (3µm from the membrane) were all Arp2/3 positive (Fig. 3D & E). In contrast, the filopodial tips of Diaph2$^{C/A}$ cells were negative for Arp2/3 antigen (Fig. 3D), whereas Arp2/3 was frequently observed along the entire shaft and at the tip of wildtype filopodia (Fig. 3E). To quantify the extent of Arp2/3 tip exclusion, we measured the distance from the tip of filopodia to the first detectable Arp2/3 signal and observed a significantly greater distance of Arp2/3 from the filopodial tip in Diaph2$^{C/A}$ cells relative to WT cells (6.2µm versus 1.4µm; p>0.0001; n = 50). In summary, by mapping the HIV budding sites at high resolution we could reach several conclusions . Firstly, HIV buds primarily enrich to cortical F-Actin structures with positive curvature. Secondly, positive curvature and/or Diaph2 activity alone are not responsible for the enrichment of HIV buds to these sites. Finally, Arp2/3-dependent cortical F-actin structures are primarily HIV positive.

<u>HIV Gag can influence Arp2/3 dependent F-Actin pathways</u>

Since HIV assembly at the PM is primarily driven by HIV-Gag, we turned to strategic Gag mutagenesis in an attempt to resolve the link of HIV assembly with cortical F-Actin structures. The HIV Gag mutant panel covered several well characterised mutants that could maintain HIV particle assembly and also binding to membrane Phosphatidylinositol (4,5)-bisphosphate (PIP2). Deletion of HIV Gag p6 and mutagenesis of the PTAP motif in p6, was used to block the recruitment of TSG101 and related ESCRT proteins involved in viral particle abscission (Fig. 4A-B). We also deleted the Nucleocapsid (NC) domain, as this has been previously proposed to mediate the interaction between HIV-Gag and F-actin [46,47]. However, since NC is required to facilitate higher order oligomerisation of Gag [48], we replaced NC with the Leucine Zipper (LZ) domain from the *Saccharomyces cerevisiae* GCN4 protein (Fig. 4C), as this rescues Gag oligomerisation and ensures particle assembly proceeds in the absence of NC [49]. Finally, given the enrichment of HIV buds on F-Actin structures with positive curvature, we further generated two HIV Gag Capsid mutants $P_{99}A$ and $EE_{75,76}AA$ (Fig. 4D & E), both of which inhibit Gag curvature at the PM but not high order Gag oligomerisation [50,51]. As Diaph2 cannot recruit HIV to F-Actin and depletion of Diaph2 actually enriched HIV-positive filopodia (Fig. S1), we utilised Diaph2^{-ve} cells and simply scored the number of filopodia per cell that were HIV positive for each viral Gag mutant. Using this approach, we observed no significant difference in viral filopodia when deleting p6, the PTAP motif in p6 or NC (Fig. 4F). However when using the $P_{99}A$ and $EE_{75,76}AA$ HIV capsid mutants (HIV curvature mutants), we observed Diaph2-depleted cells to not only lack any evident HIV buds at the PM but also their characteristic short filopodia. Instead, these cells resembled the lamellipodial phenotype observed in Diaph2^{-ve}Arp2/3^{-ve} co-depleted cells (Fig. 4G-I). This is consistent with

HIV Gag curvature mutants acting as dominant negatives for the Arp2/3-dependent short filopodial pathway. To further test that HIV curvature mutants were specifically interrupting Arp2/3 F-actin pathways and not broadly influencing all pathways that may lead to filopodial formation (eg. Formin-induced filopodia), we infected Diaph2$^{C/A}$ cells with these mutants. In this setting we observed an ability of Diaph2$^{C/A}$ to rescue filopodia formation (Fig. 4F; Movie S4). Thus filopodial pools nucleated by Arp2/3 are most affected by HIV curvature mutants and this further supports the hypothesis that HIV assembly primarily influences elements of Arp2/3 F-Actin nucleation pathway.

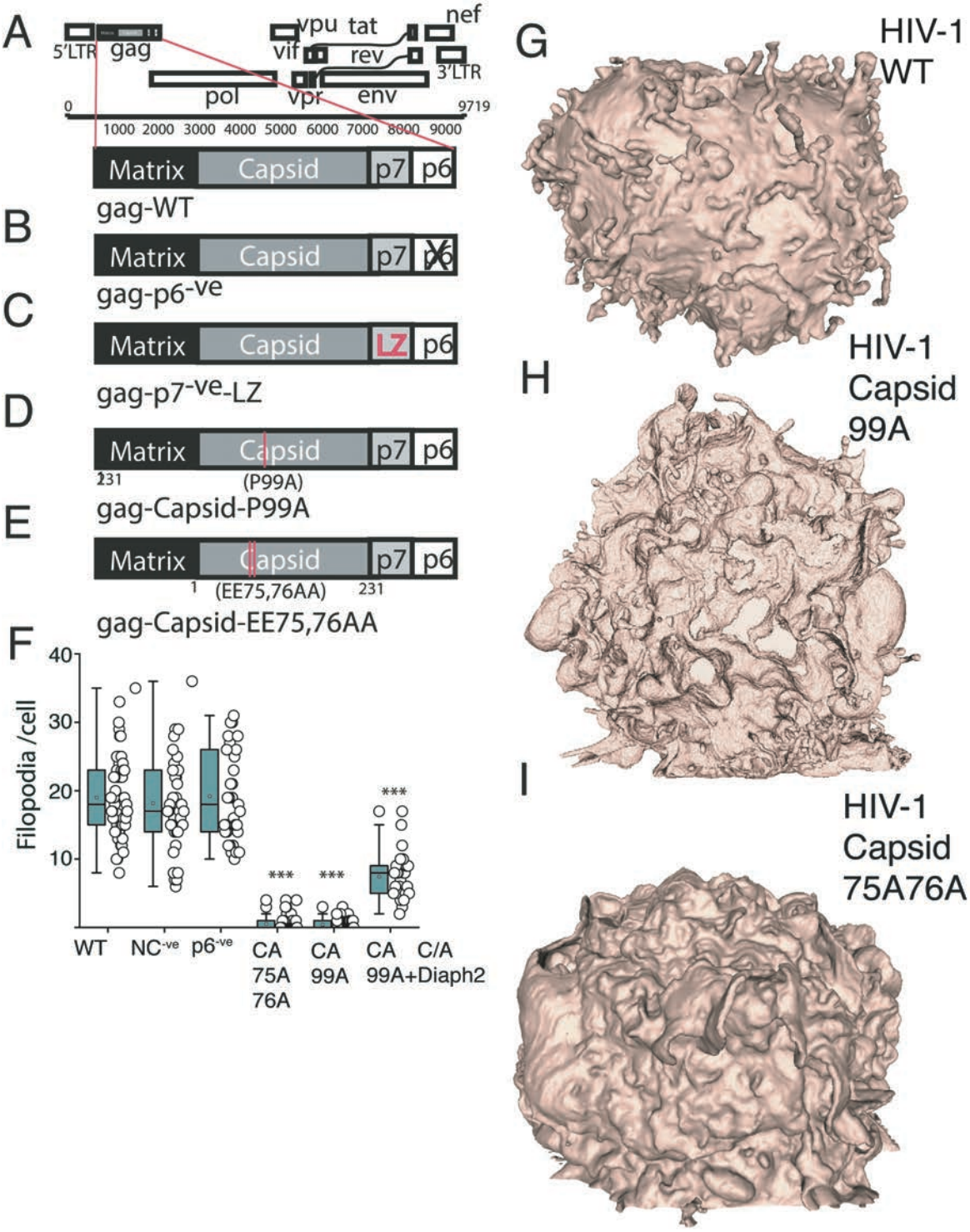

Figure 4. HIV Gag curvature mutants can impact Arp2/3 dependent cortical F-Actin

A-E HIV Gag mutants used. A. Wild type HIV Gag. B. HIV Gag late domain mutant with p6 deleted. C. NC deletion mutant with the Leucine Zipper (LZ) derived from *Saccharomyces cerevisiae* GCN4 to rescue Gag oligomerisation. D&E. HIV Gag curvature mutants D. P99A and E. EE75,76AA. F. Enumeration of filopodia per cell in Diaph2^{-ve} cell clones. ***=p<0.0001. G-H Representative FIB-SEM 3D rendered images of G. WT versus curvature mutants H. P99A and I. EE75,76AA.

The HIV proteome reveals a GTPase node associated with Arp2/3 F-Actin regulation

HIV has been previously observed to incorporate F-Actin, various actin nucleators and numerous upstream/downstream regulators within virions [52-56]. Thus, we turned to mass spectrometry analysis of purified virions to observe the footprint of cytoskeletal proteins that are present at HIV assembly sites. For this analysis we also leveraged the three distinct F-Actin cell types generated above (i.e. long-filopodia, extensive short filopodia and large lamellipodia) as across each cell type they shared the feature of HIV buds being enriched in positively curved F-Actin structures. Using this approach we identified several Arp2/3 complex subunits, alongside two major Arp2/3 regulators, the Rho-GTPases Rac1 and Cdc42, as well as their interaction partner IQGAP1. These regulators were observed across all viral proteomes, irrespective of producer cell type (Fig.5 A&B). In addition to this F-Actin signalling node, HIV virions also acquired members of the integrin and cadherin families (Fig. 5 A-B; see nodes 3 and 4, respectively). These proteins, which are involved in cell-cell adhesion, are connected to the cortical F-actin cytoskeleton both physically and via signalling pathways [57,58]. Of interest was a depletion of the cadherin node in (Fig. 5 A; node 4), as well as an increase in Arp2/3 and Cdc42 content (Fig. 5 A; node 1) in virions produced by Diaph2-deficient cells. The latter observation is not only consistent with HIV assembly preferentially proceeding alongside short Arp2/3-dependent filopodia (as observed by FIB-SEM), but also suggests that these structures are dependent on Cdc42, which is a well known filopodial regulator [10,23]. Of note, the observed decrease of Arp2/3 components in virions produced in Diaph2 and Arp2/3 co-depleted cells (Fig. 5B, node 1) is both expected and consistent with depletion of these proteins at the cellular level (Fig. S3).

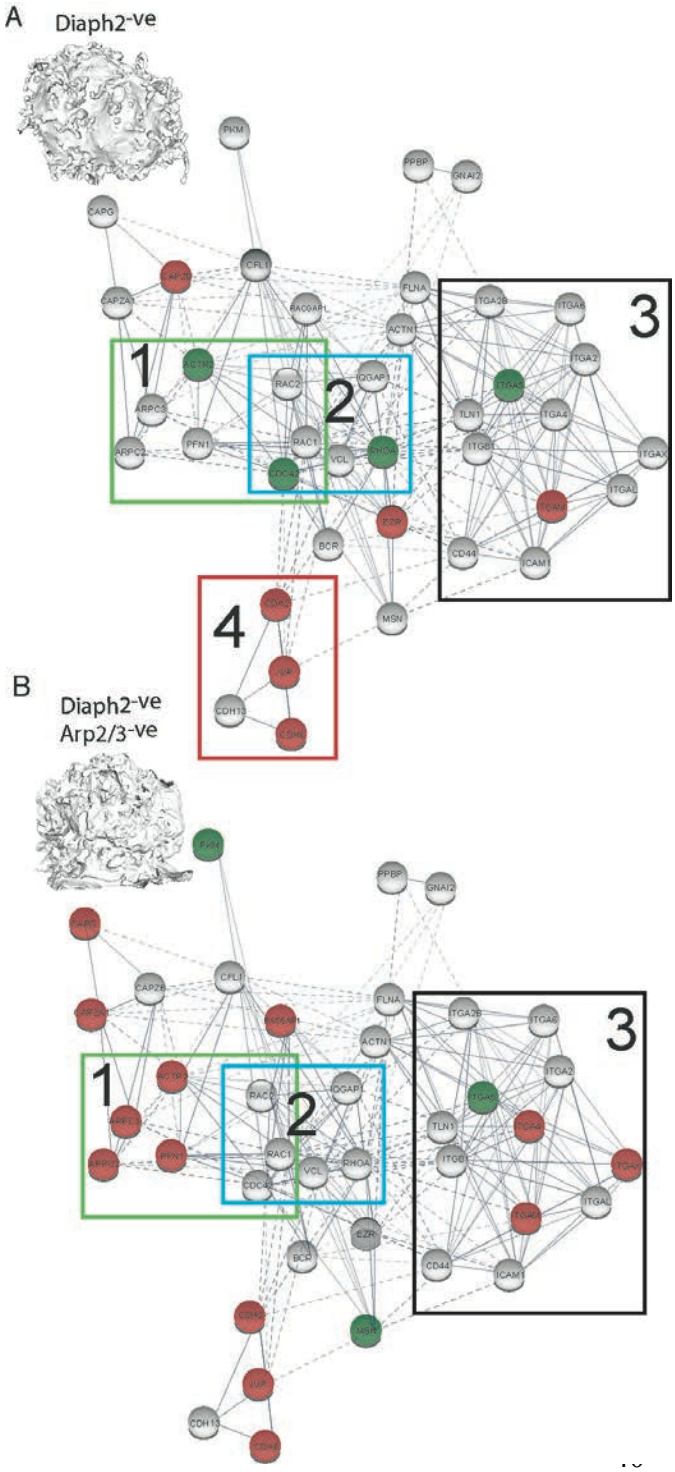

Figure 5. Cortical F-Actin regulators enriched at the final stages of HIV egress are revealed through HIV proteomics.

A-B Viral proteome analysis of proteins associated with cortical F-Actin regualtion. Proteins with increased abundance relative to untreated cells are shown in green, whereas those with relative decreased abundance are shown in red. A. Virions produced in Diaph2^{-ve} cells. 1. Highlights the Arp2/3 complex node where the amounts of ACTR2 and Cdc42 are increased in virion proteomes. 2. Indicates a GTPase node in association with IQGAP1. 3. Highlights a node of integrin and related proteins. 4. Highlights a node involved in cadherin adhesion that is downregulated upon Diaph2 depletion. B. Virions produced in Diaph2^{-ve}Arp2/3^{-ve} cells. Note that in 1. Arp2/3 components are predictably depleted compared to untreated cells, whilst in 2. the GTPase node and IQGAP1 remain unchanged.

HIV exploits the Cdc42-Arp2/3 filopodial pathway to position virus at the leading edge of cell-cell contacts.

Since Cdc42 is an important regulator of Arp2/3, a master regulator of filopodia, and it was incorporated at higher levels in virions from our Diaph2^{-ve} cells (more abundant short filopodia), we next targeted this protein for depletion. As a functional control, we targeted the homologous Rho-GTPase Rac1, best known for its role in lamellipodial regulation. We also investigated the scaffolding protein IQGAP1, which; i) is a binding partner and effector of both Cdc42 and Rac1 [59,60], and ii) plays an increasingly recognized role in actin cytoskeleton regulation [61,62], and iii) was consistently incorporated in virions in our experiments (Fig.5).

While we succeeded in generating a viable Cdc42 homozygous knockout cell line using CRISPR/Cas9 (Fig. S4). Attempts at knocking out Rac1 led to multinucleated cell populations with reduced viability, which is consistent with previous reports of Rac1 being an essential gene [63,64]. To circumvent this, we partially depleted Rac1 by shRNA, and also generated a Wave2$^{k/o}$ cell line (Fig. S4), since Wave2 is the main downstream effector of Rac1 in F-actin regulation [65,66]. While obtaining homozygous IQGAP1 knockout clones via CRISPR-Cas9 proved challenging, we were able to establish a line stringently depleted of IQGAP1 using shRNA (>99% depletion at the protein level, Fig. S3).

Initial Rac1 depletion via shRNA, revealed a greater frequency of filopodia in infected cells and secondly the generation of significantly longer and thicker filopodia when cells were infected (Fig. 6B vs A). Similarly, WAVE2$^{k/o}$ cells infected with HIV had greater propensity to form filopodia (two-fold), and these were significantly longer and thicker compared to WT cells (Fig. 6C vs A and Fig. S2), but also uninfected WAVE2$^{k/o}$ cells (Fig. S2). Together these observations suggest that HIV infection stimulates a pathway of filopodial formation that is unchecked in Rac1^{-ve} and WAVE2$^{k/o}$ cells, where the lamellipodial F-actin arm is disabled. Given the known role of Cdc42 in filopodia formation and its competing nature with the Rac1 pathway, we turned our attention to this Rho-GTPase. Importantly, Cdc42$^{k/o}$ cells were devoid of filopodia and coalesced cortical F-Actin into prominent lamellipodia, with no evident influence on F-actin when cells were HIV infected (Fig. 6D). Since IQGAP1 has been previously reported to articulate Cdc42 signaling to the cytoskeleton [62], we also assessed the role of this regulator in the filopodial context. IQGAP1-deficient cells displayed a collapse in filopodial lengths (Fig. 6E), with maintenance of HIV at the leading edge of remaining filopodia, similar to that observed in Diaph2-depleted cells. We therefore conclude that IQGAP1 can influence filopodial networks but, like Diaph2, is not required for the seeding of filopodia. To summarize our combined observations from mass spectrometry, gene silencing and high-resolution imaging, reveal that HIV infection augments a pathway of filopodia formation, and this is most evident when the lamellipodial regulators are inactivated. In contrast, removing Cdc42 completely blocked filopodia formation in a manner similar to Arp2/3 and Diaph2 co-depletion, whereas depletion of IQGAP1 or Diaph2 led to shorter filopodia. Together, our data indicates that HIV-assembly hijacks a cellular pathway that is dependent on Cdc42-Arp2/3 F-actin nucleation for filopodial seeding and IQGAP1/Diaph2 for filopodial elongation, in order to position itself at the tips of filopodia.

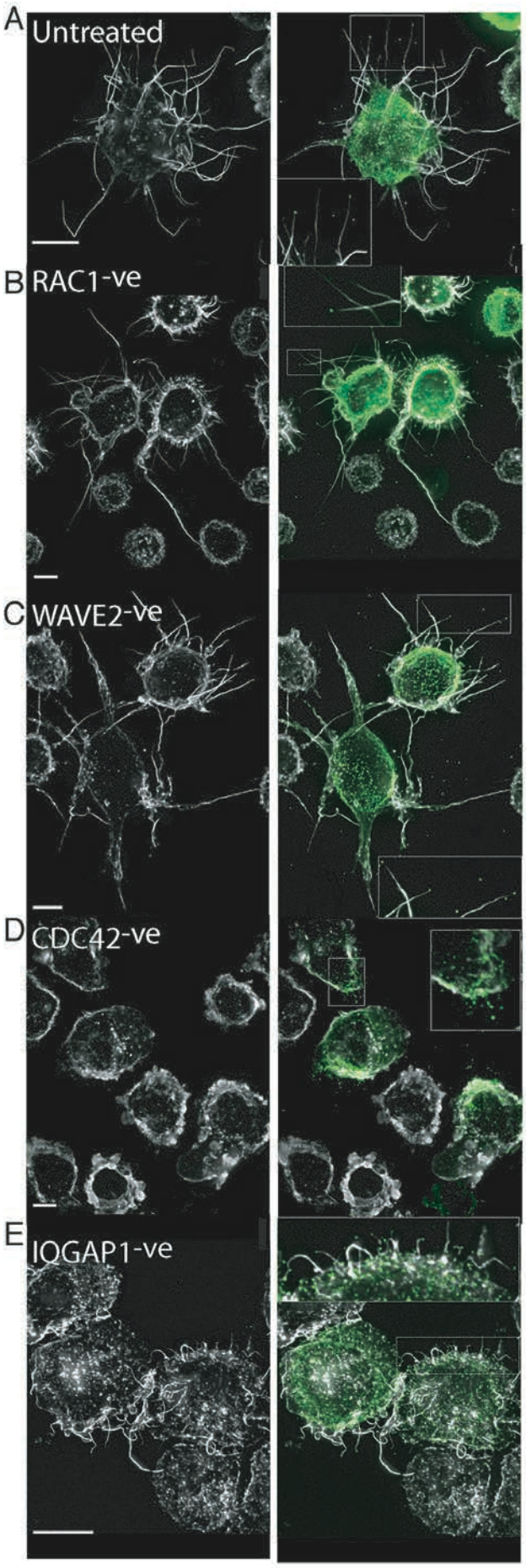

Figure 6. HIV infection and its influence on cortical F-Actin.

A. From viral proteomics, we identified a common node of actin regulators sassociated with Arp2/3-dependent filopodia and lamellipodia. Through shRNA depletion or CRISPR-Cas9 knockout, we generated clonal cell populations depleted of various actin regulators. B-C Lamellipodial regulators. B. Rac1^{-ve} and C. WAVE2$^{k/o}$. D. Cdc42$^{k/o}$ (filopodial regulator). E. IQGAP1^{-ve}. A. Represents the untreated control. All cells were infected with HIV iGFP (green) and then counterstained with phalloidin Alexa-647 (white). All scale bars are at 5µm. Inset magnifications reveal HIV at the leading edge of filopodial structures. Note in Rac1^{-ve} and WAVE2$^{k/o}$ images the extensive filopodial networks only present in HIV infected (green) cells (see Fig. S2 for formal quantification).

HIV cell-cell transfer is dependent on an intact Cdc42-IQGAP1-Arp2/3 pathway

Given the continuum of phenotypes observed in our abovementioned observations, we tested their impact on the late stages of the viral life cycle in the context of viral spread. For free virus release, we enumerated HIV particles accumulating in the supernatant as a measure of budding. As HIV spread can also proceed through direct cell-cell contacts, we further tested the ability of HIV to spread cell to cell by coincubating infected donor cells with permissive target cells. Using these approaches, we could determine if the generic lack of a cortical F-Actin structure or a specific F-Actin pathway is essential for HIV budding and/or cell-cell transfer.

Disruption of either the Rac1-WAVE2 pathway (lamellipodia) or Cdc42-IQGAP1 pathway (filopodia) both impaired free HIV budding, as indicated by significantly lower viral particle counts in the supernatant from cells depleted of these regulators, compared to untreated cells (Fig. 7 B). However, impaired release of free HIV did not predict outcomes for cell-cell HIV transfer. For cells with disabled Rac1/WAVE2 ($Rac1^{-ve}$, $Wave2^{k/o}$ cells) cell-cell HIV transfer persisted (Fig. 7 A&B), despite the decreased free virus budding ability. In contrast, disruption of the Cdc42/IQGAP1 axis (Cdc42k/o and IQGAP1-ve cells) impacted both HIV budding and cell-cell transfer (Fig. 7 A&B). These observations suggest that while normal actin dynamics are important for free virus release, Cdc42 and IQGAP1 are specifically required for cell-cell HIV transfer, whereas Rac1/Wave2 are not. To further test this hypothesis in the setting of primary CD4 T cell targets, we focussed cell-cell transfer assays with disruption of the Rac1-WAVE2 pathway versus disruption of Cdc42-IQGAP1. In this setting, we further tested the efficiency of cell-cell spread by limiting dilution of the infected donors into primary CD4 T cell co-cultures. Using this approach, we observed almost complete loss of cell-cell HIV transfer in $Cdc42^{k/o}$ and $IQGAP1^{-ve}$ clones, whereas cell-cell transfer persisted in $Rac1^{-ve}$, $Wave2^{k/o}$ clones, albeit slightly lower than in WT cells (Fig. 7C). In cells lacking filopodia (CDC42 and IQGAP1), one immediate mechanism for lack of viral transfer could be the culmination of a limited contact capacity with the cells immediate microenvironment. To test this hypothesis, we enumerated accumulative cell to cell contacts (Fig. 7D) and later target cell engagement (Fig. 7E) in wild type, $IQGAP1^{-ve}$ and $WAVE2^{k/o}$ cells. $IQGAP1^{-ve}$ cells were observed to have significantly lower overall contacts and also engaged fewer cell targets. Whilst this addresses the lowered ability of cells without filopodia to participate in cell-cell transfer, it does not address the address the paradox of persistent cell-cell HIV transfer, despite reduced viral budding in cells with augmented filopodia. To observe this latter phenotype we turned to live imaging of HIV infected $Wave2^{k/o}$ clones to observe F-Actin dynamics during viral transfer. As expected, HIV infected $Wave2^{k/o}$ clones displayed extensive and dynamic filopodial networks (Movies S5 & S6). Donor-target cell interactions were often guided by filopodial activity. In $IQGAP1^{-ve}$ cells we observed a distinct lack of this filopodial guiding and this led to signficantly lower cell-cell contacts and subsequent conjugate formation, when compared to filopodially active wild type and $WAVE2^{k/o}$ cells (Fig. 7D & E). Whilst this mechanistically can explain a lack of cell-cell transfer in $IQGAP1^{-ve}$ cells, it does not explain how in cells enriched with HIV filopodia, where HIV budding is arrested ($WAVE2^{k/o}$ cells), viral infection can proceed if cell-cell contact are made. To resolved this further, we observed later interactions $WAVE2^{k/o}$ cells where filopodial networks are augmented following HIV infection. Filopodia initially persisted in early cell-cell conjugates, yet we routinely observed collapse of filopodial networks immediately preceding VS formation and HIV-GFP transfer to the opposing target cell (Fig. 7 F and Movie S6). As a surrogate of filopodial activity, we quantified this as membrane complexity through calculation of cellular circularity. In this setting, cells with extensive filopodial networks were observed to have low circularity, whilst cells with no filopodial activity were observed to have high score in circularity. Measurements of Gag-polarisation over time then established measurements of the seeding of the VS and

release of GFP into the neighbouring target was used to mark the final stage of VS maturation that culminated in viral transfer. Using this quantification in the live cell movie acquistions (7 F &G), we observe cells engaged in cell-cell contact to approach a circularity of 1 (i.e. Cells collapsing their filopodial networks) just prior to the final stages of viral transfer, as marked intitially by Gag polarisation and then subsequently observed in cytoplasmic transfer to the neighbouring cell (7G).

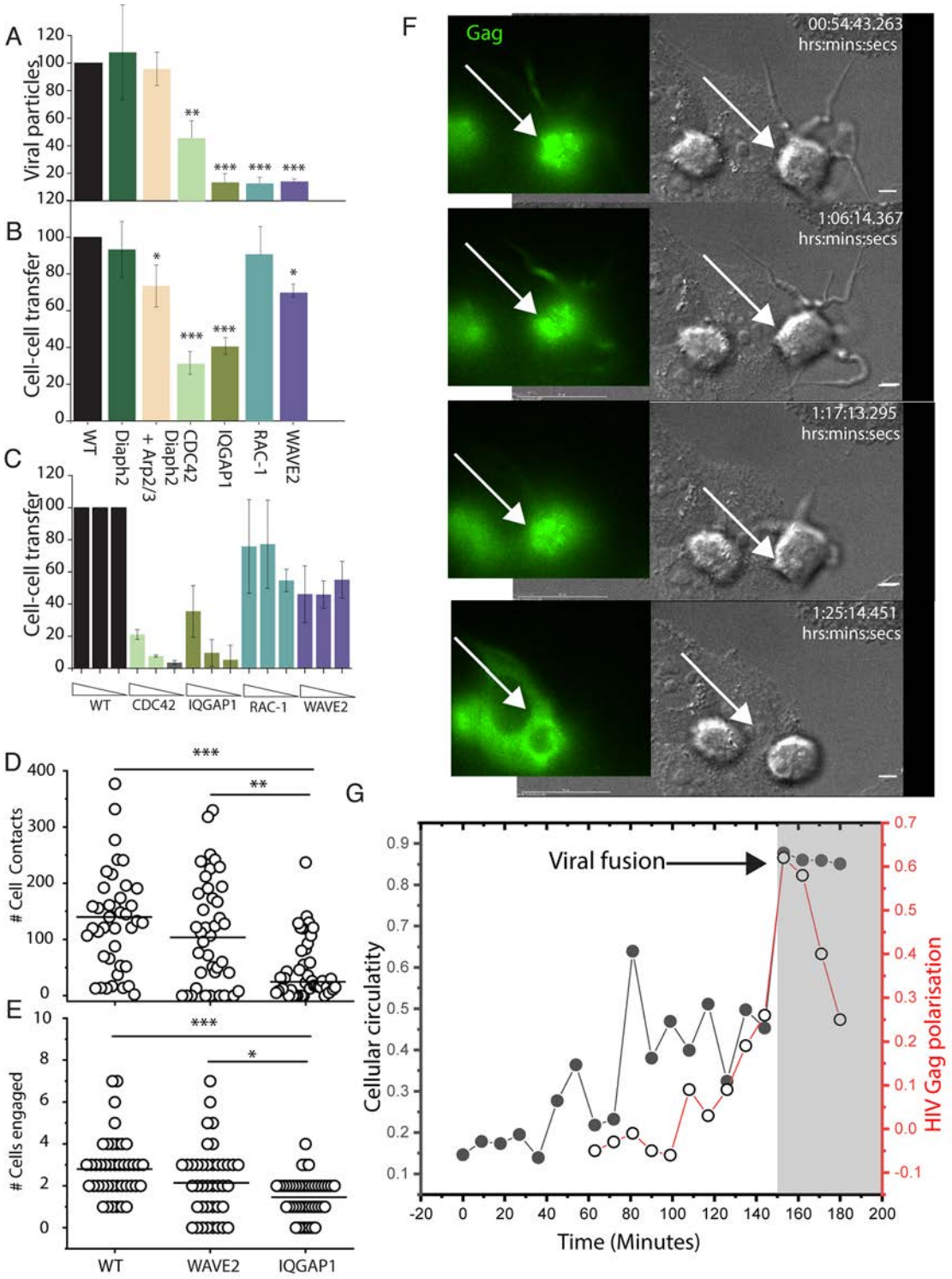

Figure 7. HIV spread is dependent on Cdc42 and IQGAP1

A. All cells are infected with pHIVNL43iGFP and normalised to 5% infection on day 3. After normalisation, cell supernatants are collected over a 24 hour period and GFP positive HIV particles are spinoculated onto 96-well glass plates coated with poly-L-lysine. Absolute viral particle counts are determined by high-resolution fluoresecence microscopy per 4 fields of view. Herein the data is presented as a relative count [(virion count/virion count in WT control)*100]. B. HIV infected cells as normalised in A. are then co-cultured at a ratio of 1:5 with HIV-permissive TZMBl targets. C. Infected cells are co-cultured with primary CD4 target T-cells at limiting dilutions. Dilution steps correspond to 5%, 1% and 0.2% infected cells in the donor population. Exposure to virus from infected cells is limited to 24 hours, after which an entry inhibitor BMS806 is added to prevent further viral spread. A-C. Data indicates the mean and standard deviation from 3 independent experiments. In C, primary recipient CD4 T cells were sourced from independent blood donors. D) The cumulative number of contacts between each infected donor cell and any uninfected target cells (TZM-bl) over 3 hours. E) same as D but only the first contact with each distinct target cell is counted. F) Representative example of a time-lapse series from D-E. Cells are infected with HIViGFP, allowing real-time visualization of Gag. G) At the virological synapse, donor-cell circularity was used to enumerate lack of membrane protrusions (ie. Lack of filopodia) in parallel with Gag polarization. In grey shading are the time points where GFP cytoplasmic transfer (ie. Viral fusion) is observed. * $p<0.01$, **$p<0.001$, ***$p<0.0001$.

To conclude, in regard to F-Actin-dependent HIV spread we make two important observations. Firstly, whilst viral budding is sensitive to depletion of the Arp2/3 regulators Rac1/WAVE2 and Cdc42/IQGAP1, cell-cell spread is primarily dependent on Cdc42/IQGAP1. Whilst this may be dependent on limited HIV filopodial activity decreasing cell-cell contacts, we cannot rule out additional viral blocks at the VS if IQGAP1 is removed. Secondly, although HIV manipulates and enhances Cdc42/IQGAP1-dependent filopodia, which help mediate early donor-target cell contacts, Cdc42 may be inactivated at later stages of cell-cell HIV transfer, as suggested by collapse of filopodial networks during VS progression that culminates in viral delivery.

Discussion

The corruption of cortical F-Actin by HIV has remained elusive, with evidence both for and against its role in budding and cell-cell viral spread [16,20,33,67]. Through systematic depletion of various F-Actin regulators, combined with viral mutagenesis and high-resolution imaging, we were able to illuminate the intersection of HIV egress with cortical F-Actin and conclude this is primarily associated with the Cdc42-IQGAP1-Arp2/3 pathway.

Our primary aim herein was to understand how HIV egress was spatiotemporally connected to a continuum of cortical F-actin structures that dynamically regulated in leukocytes. Whilst many prior studies have mapped F-Actin pathways in cell-free systems, the challenge herein was to map F-Actin pathways and how they influenced not only the live virus, but also in a cellular & cytoskeletal setting that was consistent with that of the immune system. Whilst many F-Actin regulators are common across cells, F-Actin regulation in leukocytes is unique and enables a rapidly changing canvas of F-Actin polymers to coordinate their roles in the immune response. Processes such as chemotaxis, promisicous cell-cell scanning and later stable cell-cell contacts that mediate downstream immune responses through immunological synapses are all processes dependent on dynamic cortical F-Actin. So in discussion of the how F-Actin influences HIV egress, we need to emphasise that firstly this needs to be focussed on cells of hemopoetic lineage and secondly that each F-Actin pathway appears temporally and as such we need to frame each pathway when it dominates to observe how it would influence HIV at that specific point in time. In discussion we will address this at two levels. Firstly, HIV's time at the leading edge of protruding F-Actin structures, when cells explore their immediate environments. Secondly, when infected cells select and engage in longer stable contacts.

In exploiting the power of FIB-SEM imaging, we observed HIV buds to be enriched to the leading edge of the PM where cortical F-actin structures induce strong positive curvature. However, curvature and/or formin activity alone were not sufficient to position HIV at the tips of filopodia. Thus, other actin regulators associated with membrane curvature must be involved. Our observations herein that HIV infection specifically enhances Cdc42-Arp2/3-dependent filopodia, supports a mechanism of action that corrupts this pathway of actin nucleation. While it is conceivable that the curvature provided by HIV during budding could itself drive filopodia formation (e.g by direct recruitment/activation of Cdc42/Arp2/3 [68,69], we deem more likely that the virus hijacks a pre-existing cellular pathway that is dependent on curvature and that involves these regulators. We base this reasoning three-fold. Firstly on uninfected myeloid cells there are similar long filopodia (albeit uncapped with HIV). Secondly most filopodia in infected cells are HIV-capped [18]. If HIV would provide an independent mechanism of filopodia formation, both structures would be expected to coexist, whereas in reality HIV-capped filopodia in infected cells predominate. Thirdly and finally, HIV curvature mutants had a dominant negative effect on all filopodia, indicating i) a functional overlap of the viral and cellular pathways of filopodia formation, and ii) a critical role of Gag in hijacking of these structures. Whilst our work herein was in review, Sabo and colleagues observed HIV Gag to directly interact with IQGAP1 [70]. This observation is consistent with our observations herein at several levels. Firstly, as IQGAP1 binds to Cdc42 and stabilizes it in its active conformation to drive filopodia formation [62]. Secondly, as IQGAP1 also facilitates assembly of multiprotein complexes that spatially link Cdc42, Arp2/3 and formins [61,71,72]. This late complex is consistent with how HIV is associated with a filopodial structure that is firstly nucleated by CDC42, but secondly elongated by the formin Diaph2. Finally, given the role of positive curvature in filopodia biogenesis, consumption of IQGAP1 by HIV Gag into an area of neutral curvature, is entirely consistent with HIV Gag curvature mutants acting as dominant

negative constructs for CDC42-Arp2/3 driven filopodia. Whilst the resolution of the multi-layered viral and cellular pathways that gives birth to HIV filopodia are now becoming clearer, the role of this hybrid viral and cellular structure now needs discussion. In many other enveloped viruses, filopodia have been associated with the ability to mediate cell-cell viral transfer [73-77]. Yet, this latter concept is at odds at our observations of viral egress. In many settings where F-Actin regulation is significantly perturbed by the presence of high cortical F-Actin concentrations in either extensive lammelipodial or filopodial pools, so to is viral egress. The most evident is when HIV filopodial networks are formed during Rac1 and Wave2 depletion. In that setting, the removal of Rac1 would not only bias signalling to CDC42, but with IQGAP1 recruited by HIV Gag, CDC42 would be maintained in an active GTP bound state [78]. This is entirely consistent with its role in filopodial formation but also its augmentation by HIV Gag-IQGAP1 during infection. Whilst arrest of viral HIV buds in a F-Actin structure may be a simple function of distance that this structure projects immature HIV from the plasma membrane, the role of the virus in this setting is seems counter intuitive, as a virus that cannot undergo absciscion at the membrane cannot subsequently mature [79] and as such this cannot directly contribute to viral spread. Yet in this setting, we hypothesise leading edge structures positive with HIV can indeed indirectly contribute to cell-cell spread. For instance, we have previously observed HIV-Filopodia to mediate hundreds of contacts per hour between relevant primary HIV target cells, with filopodial activity often preceding VS formation [18]. The latter is in agreement with previous observations that filopodia and/or dendrites may commonly serve as precursors for biological synapses [80-84]. So in this setting, the virus at the leading edge of protruding F-Actin structures may indeed be hard-wired to coordinate the initial pre-synaptic contacts. Whilst these HIV buds would be sacrificed during this process, a secondary wave of budding (from another pool of HIV Gag) would proceed once stable cell-cell contacts matured. So to conclude, HIV's time in this setting is focussed at the leading edge of a cell contacting its surrounding environment. Release of virus is lowered, increasing the half life of HIV's corruption of the leading edge to enable initial cell-cell contacts. This is consistent with our observations herein where cells with intact CDC42 and IQGAP1 expression mediating greater numbers of contacts that lead to a greater number of committed cell-cell engagements in live cell cultures (this model is now visually summarised in Fig. 8A) and result in the transfer of viral infection.

Now lets consider the second stage of viral transfer and the regulation required to close cell to cell contacts and final release of the virus for infection across the synaptic cleft. In contrast, we observed cell-cell spread of HIV to be primarily dependent on Cdc42 and IQGAP1 but showed tolerance to depletion of Rac1/Wave2, despite a similar impact of all regulators on free virus budding. Whilst the generation of a F-Actin structure driven by CDC42 and IQGAP1 can dictate early cell-cell contacts, their subsequent role during the maturation of the VS is potentially temporally and mechanistically complex. This complexity is directly a consequence of the role of IQGAP1 in many cellular events, including scaffolding proteins during cell-cell adhesion[85,86], the potential influence on abscission pathways by directly binding to TSG101 [87], and its abovementioned role in Arp2/3 F-Actin polymerisation [88]. Whilst complex, the maturation and function of the VS requires all of the above events and we hypothesise IQGAP1 provides the scaffolding center that enables coordinated cell-cell adhesion and F-Actin polymerisation in a manner that facilitates viral budding/"release" into the synapse. Mechanistically, the maturation of the immunological synapse (IS) proceeds in a similar manner to the viral synapse (VS). In both structures a supramolecular activation cluster forms (SMAC) at the contact site between cells. At the center of the SMAC (cSMAC), clearance of F-Actin proceeds alongside IQGAP1 [89-91], where they both coallese to a peripheral ring of F-Actin (pSMAC and dSMAC) alongside such as ICAM1 [91]. In this setting F-Actin

remodelling at the IS is driven by CDC42 [90]. In addition, the abscission machinery TSG101 is retained and is essential not only for the development of the cSMAC but also for subsequent abscission events that liberate vesicles at the IS [92]. At the molecular level vesicle secretion is dictated by the the switching roles of CDC42 and IQGAP1, as the partnering of these two proteins in their F-Actin stimulatory form, active GTP-CDC42 bound to the C-Terminus if IQGAP1, inhibits exocytosis/ vesicle secretion [93]. Based on our observations herein, we would support a similar model for CDC42-IQGAP1 at the VS, where initial adhesive events mature into a structure that favours the release of HIV at the cSMAC. In support of this, as in exocytosis inhibition, F-Actin active GTP-CDC42-IQGAP1 complexes we observe also observe to arrest viral release. To conclude, HIV's relationship with F-Actin is indeed complex and the role of F-Actin regulation in HIV spread requires appreciation of time and space for an infected cell.

Shadowing and highjacking the Cdc42-IQGAP1-Arp2/3 actin regulatory axis is not a unique feature of HIV. Nascent viral buds have also been observed at the tips of filopodia-like structures for other types of viruses [94-99], and numerous intracellular pathogens are known to exploit Rho-GTPases and the unique ability of the Arp2/3 complex to promote formation of specialized cortical F-actin membrane protrusions that facilitate cell-cell infection spread [100-104]. Similarly, IQGAP1 is a prominent target of microbial manipulation and this is closely related to its ability to modulate the actin cytoskeleton (reviewed in [105]). Several viruses bind IQGAP1 either directly (via interactions with the viral matrix protein) or indirectly (via common binding partners) and this has important consequences for viral assembly, budding and/or pathogenesis [21,96,106-109]. For HIV, recent studies by Sabo and colleagues [70], have observed biochemically IQGAP1 interactions with NC & p6 elements of HIV Gag. In this study they support a role for IQGAP1 in negative regulation of HIV Gag trafficking and subsequent HIV-budding [70]. Whilst our observations readily support a role for IQGAP1 in influencing HIV budding, we did not observe this to be a consequence of negative regulation of Gag trafficking and docking to the membrane. For instance near complete removal of IQGAP1 did not increase viral budding and egress, but rather led to inhibition thereof. In light of our observations herein and those recently published whilst our study was in review [70], we would conclude that as IQGAP1 is a scaffolding protein with many binding partners, it is not surprising that HIV Gag has many different fates depending on each cell type it is expressed in and what functions that cell type maybe engaged over the time the cells were sampled. Importantly, we do readily support a role for IQGAP1 in the viral life cycle and this readily supports recent observations by this team.

Overall, we propose that HIV has evolved to highjack a specific node of F-actin regulation that positions outgoing virus at the leading edge of cortical F-actin structures. Since filopodia play an important role in scanning of the microenvironment and mediating immune cell interactions, their corruption is beneficial to the virus because it biases the first line of cell-cell contacts towards HIV spread, e.g. by providing enhanced adhesion and specificity to CD4+ target cells. However, as these contacts form and the VS matures, the relationship of HIV with F-Actin must change to enable viral release. We conclude that manipulation of the Cdc42-IQGAP1-Arp2/3 actin regulatory node is essential for corruption of cellular filopodia to facilitate cell-cell HIV spread, and propose a key role for IQGAP1 in integrating signals of F-actin regulation and viral abscission to strategically enhance HIV egress at sites of productive cell-cell contact. Moving forward, greater spatiotemporal resolution of this final release event is needed and will give further insight into why many pathogens like HIV have evolved to interact with IQGAP1 and its binding partners.

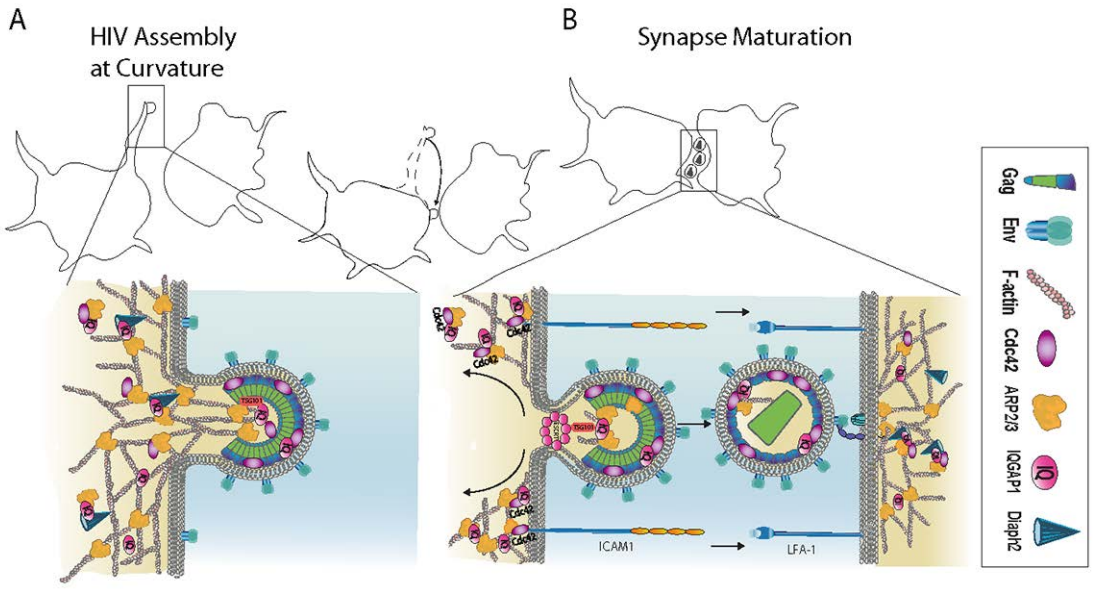

Figure 8. Proposed model of spatio-temporal regulation of F-Actin during HIV egress. A. With probing and tethering activity corrupted by HIV buds, the F-actin structures at this phase enable pre-synpatic events (cell contacts and initial adhesion). B. Following cell-cell engagement, the viral synapse matures. This leads to two important outcomes. Firstly, similar to that observed at the immunological synapse [90] Cdc42-F-Actin activity is altered and transitions from filopodial biogenesis to cell-cell adhesion required for HIV release (as observed when cells collapse filopodia just prior to HIV fusion). During this change we hypothesise IQGAP1 being directly involved through providing a scaffolding center needed temporally coordinate binding not only to HIV Gag, but also providing feedback to other binding partners including Cdc42 and TSG101. Whilst the observations herein and recently by others [70], initially supports this model, future work will be key in understanding the switching nature of IQGAP1 and how F-Actin and CDC42 influences its role in the final stages of viral absciscion and transfer.

References

1. Leavitt, J.; Leavitt, A.; Attallah, A.M. Dissimilar modes of expression of beta- and gamma-actin in normal and leukemic human T lymphocytes. *The Journal of biological chemistry* **1980**, *255*, 4984-4987.
2. Huppa, J.B.; Davis, M.M. T-cell-antigen recognition and the immunological synapse. *Nature reviews. Immunology* **2003**, *3*, 973-983, doi:10.1038/nri1245.
3. Grakoui, A.; Bromley, S.K.; Sumen, C.; Davis, M.M.; Shaw, A.S.; Allen, P.M.; Dustin, M.L. The immunological synapse: a molecular machine controlling T cell activation. *Science (New York, N.Y.)* **1999**, *285*, 221-227, doi:10.1126/science.285.5425.221.
4. Chesarone, M.A.; Goode, B.L. Actin nucleation and elongation factors: mechanisms and interplay. *Current opinion in cell biology* **2009**, *21*, 28-37, doi:10.1016/j.ceb.2008.12.001.
5. Campellone, K.G.; Welch, M.D. A nucleator arms race: cellular control of actin assembly. *Nature reviews. Molecular cell biology* **2010**, *11*, 237-251, doi:10.1038/nrm2867.
6. Egile, C.; Rouiller, I.; Xu, X.P.; Volkmann, N.; Li, R.; Hanein, D. Mechanism of filament nucleation and branch stability revealed by the structure of the Arp2/3 complex at actin branch junctions. *PLoS biology* **2005**, *3*, e383, doi:10.1371/journal.pbio.0030383.
7. Robinson, R.C.; Turbedsky, K.; Kaiser, D.A.; Marchand, J.B.; Higgs, H.N.; Choe, S.; Pollard, T.D. Crystal structure of Arp2/3 complex. *Science (New York, N.Y.)* **2001**, *294*, 1679-1684, doi:10.1126/science.1066333.
8. Chesarone, M.A.; DuPage, A.G.; Goode, B.L. Unleashing formins to remodel the actin and microtubule cytoskeletons. *Nature reviews. Molecular cell biology* **2010**, *11*, 62-74, doi:10.1038/nrm2816.
9. Aspenstrom, P. The Intrinsic GDP/GTP Exchange Activities of Cdc42 and Rac1 Are Critical Determinants for Their Specific Effects on Mobilization of the Actin Filament System. *Cells* **2019**, *8*, doi:10.3390/cells8070759.
10. Nobes, C.D.; Hall, A. Rho, rac, and cdc42 GTPases regulate the assembly of multimolecular focal complexes associated with actin stress fibers, lamellipodia, and filopodia. *Cell* **1995**, *81*, 53-62, doi:10.1016/0092-8674(95)90370-4.
11. Lifson, J.D.; Feinberg, M.B.; Reyes, G.R.; Rabin, L.; Banapour, B.; Chakrabarti, S.; Moss, B.; Wong-Staal, F.; Steimer, K.S.; Engleman, E.G. Induction of CD4-dependent cell fusion by the HTLV-III/LAV envelope glycoprotein. *Nature* **1986**, *323*, 725-728, doi:10.1038/323725a0.
12. Phillips, D.M.; Bourinbaiar, A.S. Mechanism of HIV spread from lymphocytes to epithelia. *Virology* **1992**, *186*, 261-273, doi:10.1016/0042-6822(92)90080-9.
13. Jolly, C.; Kashefi, K.; Hollinshead, M.; Sattentau, Q.J. HIV-1 cell to cell transfer across an Env-induced, actin-dependent synapse. *The Journal of experimental medicine* **2004**, *199*, 283-293, doi:10.1084/jem.20030648.
14. Sundquist, W.I.; Krausslich, H.G. HIV-1 assembly, budding, and maturation. *Cold Spring Harbor perspectives in medicine* **2012**, *2*, a006924, doi:10.1101/cshperspect.a006924.
15. Garrus, J.E.; von Schwedler, U.K.; Pornillos, O.W.; Morham, S.G.; Zavitz, K.H.; Wang, H.E.; Wettstein, D.A.; Stray, K.M.; Cote, M.; Rich, R.L., et al. Tsg101 and the vacuolar protein sorting pathway are essential for HIV-1 budding. *Cell* **2001**, *107*, 55-65, doi:10.1016/s0092-8674(01)00506-2.

16. Gladnikoff, M.; Shimoni, E.; Gov, N.S.; Rousso, I. Retroviral assembly and budding occur through an actin-driven mechanism. *Biophysical journal* **2009**, *97*, 2419-2428, doi:10.1016/j.bpj.2009.08.016.
17. Carlson, L.A.; de Marco, A.; Oberwinkler, H.; Habermann, A.; Briggs, J.A.; Krausslich, H.G.; Grunewald, K. Cryo electron tomography of native HIV-1 budding sites. *PLoS pathogens* **2010**, *6*, e1001173, doi:10.1371/journal.ppat.1001173.
18. Aggarwal, A.; Iemma, T.L.; Shih, I.; Newsome, T.P.; McAllery, S.; Cunningham, A.L.; Turville, S.G. Mobilization of HIV spread by diaphanous 2 dependent filopodia in infected dendritic cells. *PLoS pathogens* **2012**, *8*, e1002762, doi:10.1371/journal.ppat.1002762.
19. Ladinsky, M.S.; Kieffer, C.; Olson, G.; Deruaz, M.; Vrbanac, V.; Tager, A.M.; Kwon, D.S.; Bjorkman, P.J. Electron tomography of HIV-1 infection in gut-associated lymphoid tissue. *PLoS pathogens* **2014**, *10*, e1003899, doi:10.1371/journal.ppat.1003899.
20. Ospina Stella, A.; Turville, S. All-Round Manipulation of the Actin Cytoskeleton by HIV. *Viruses* **2018**, *10*, doi:10.3390/v10020063.
21. Lu, J.; Qu, Y.; Liu, Y.; Jambusaria, R.; Han, Z.; Ruthel, G.; Freedman, B.D.; Harty, R.N. Host IQGAP1 and Ebola virus VP40 interactions facilitate virus-like particle egress. *Journal of virology* **2013**, *87*, 7777-7780, doi:10.1128/jvi.00470-13.
22. Jolly, C.; Mitar, I.; Sattentau, Q.J. Requirement for an intact T-cell actin and tubulin cytoskeleton for efficient assembly and spread of human immunodeficiency virus type 1. *Journal of virology* **2007**, *81*, 5547-5560, doi:10.1128/jvi.01469-06.
23. Mattila, P.K.; Lappalainen, P. Filopodia: molecular architecture and cellular functions. *Nature reviews. Molecular cell biology* **2008**, *9*, 446-454, doi:10.1038/nrm2406.
24. Lehtimaki, J.; Hakala, M.; Lappalainen, P. Actin Filament Structures in Migrating Cells. *Handbook of experimental pharmacology* **2017**, *235*, 123-152, doi:10.1007/164_2016_28.
25. Guo, F.; Debidda, M.; Yang, L.; Williams, D.A.; Zheng, Y. Genetic deletion of Rac1 GTPase reveals its critical role in actin stress fiber formation and focal adhesion complex assembly. *The Journal of biological chemistry* **2006**, *281*, 18652-18659, doi:10.1074/jbc.M603508200.
26. Steffen, A.; Ladwein, M.; Dimchev, G.A.; Hein, A.; Schwenkmezger, L.; Arens, S.; Ladwein, K.I.; Margit Holleboom, J.; Schur, F.; Victor Small, J., et al. Rac function is crucial for cell migration but is not required for spreading and focal adhesion formation. *Journal of cell science* **2013**, *126*, 4572-4588, doi:10.1242/jcs.118232.
27. Yamazaki, D.; Suetsugu, S.; Miki, H.; Kataoka, Y.; Nishikawa, S.; Fujiwara, T.; Yoshida, N.; Takenawa, T. WAVE2 is required for directed cell migration and cardiovascular development. *Nature* **2003**, *424*, 452-456, doi:10.1038/nature01770.
28. Wu, C.; Asokan, S.B.; Berginski, M.E.; Haynes, E.M.; Sharpless, N.E.; Griffith, J.D.; Gomez, S.M.; Bear, J.E. Arp2/3 is critical for lamellipodia and response to extracellular matrix cues but is dispensable for chemotaxis. *Cell* **2012**, *148*, 973-987, doi:10.1016/j.cell.2011.12.034.
29. Suraneni, P.; Rubinstein, B.; Unruh, J.R.; Durnin, M.; Hanein, D.; Li, R. The Arp2/3 complex is required for lamellipodia extension and directional fibroblast cell migration. *The Journal of cell biology* **2012**, *197*, 239-251, doi:10.1083/jcb.201112113.
30. Young, L.E.; Heimsath, E.G.; Higgs, H.N. Cell type-dependent mechanisms for formin-mediated assembly of filopodia. *Molecular biology of the cell* **2015**, *26*, 4646-4659, doi:10.1091/mbc.E15-09-0626.

31. Eugenin, E.A.; Gaskill, P.J.; Berman, J.W. Tunneling nanotubes (TNT) are induced by HIV-infection of macrophages: a potential mechanism for intercellular HIV trafficking. *Cellular immunology* **2009**, *254*, 142-148, doi:10.1016/j.cellimm.2008.08.005.
32. Bourinbaiar, A.S.; Phillips, D.M. Transmission of human immunodeficiency virus from monocytes to epithelia. *Journal of acquired immune deficiency syndromes* **1991**, *4*, 56-63.
33. Pearce-Pratt, R.; Malamud, D.; Phillips, D.M. Role of the cytoskeleton in cell-to-cell transmission of human immunodeficiency virus. *Journal of virology* **1994**, *68*, 2898-2905.
34. Welch, M.D.; DePace, A.H.; Verma, S.; Iwamatsu, A.; Mitchison, T.J. The human Arp2/3 complex is composed of evolutionarily conserved subunits and is localized to cellular regions of dynamic actin filament assembly. *The Journal of cell biology* **1997**, *138*, 375-384, doi:10.1083/jcb.138.2.375.
35. Higgs, H.N.; Peterson, K.J. Phylogenetic analysis of the formin homology 2 domain. *Molecular biology of the cell* **2005**, *16*, 1-13, doi:10.1091/mbc.e04-07-0565.
36. Breitsprecher, D.; Goode, B.L. Formins at a glance. *Journal of cell science* **2013**, *126*, 1-7, doi:10.1242/jcs.107250.
37. Narayan, K.; Danielson, C.M.; Lagarec, K.; Lowekamp, B.C.; Coffman, P.; Laquerre, A.; Phaneuf, M.W.; Hope, T.J.; Subramaniam, S. Multi-resolution correlative focused ion beam scanning electron microscopy: applications to cell biology. *Journal of structural biology* **2014**, *185*, 278-284, doi:10.1016/j.jsb.2013.11.008.
38. Narayan, K.; Subramaniam, S. Focused ion beams in biology. *Nature methods* **2015**, *12*, 1021-1031, doi:10.1038/nmeth.3623.
39. Felts, R.L.; Narayan, K.; Estes, J.D.; Shi, D.; Trubey, C.M.; Fu, J.; Hartnell, L.M.; Ruthel, G.T.; Schneider, D.K.; Nagashima, K., et al. 3D visualization of HIV transfer at the virological synapse between dendritic cells and T cells. *Proceedings of the National Academy of Sciences of the United States of America* **2010**, *107*, 13336-13341, doi:10.1073/pnas.1003040107.
40. Bennett, A.E.; Narayan, K.; Shi, D.; Hartnell, L.M.; Gousset, K.; He, H.; Lowekamp, B.C.; Yoo, T.S.; Bliss, D.; Freed, E.O., et al. Ion-abrasion scanning electron microscopy reveals surface-connected tubular conduits in HIV-infected macrophages. *PLoS pathogens* **2009**, *5*, e1000591, doi:10.1371/journal.ppat.1000591.
41. Alberts, A.S. Identification of a carboxyl-terminal diaphanous-related formin homology protein autoregulatory domain. *The Journal of biological chemistry* **2001**, *276*, 2824-2830, doi:10.1074/jbc.M006205200.
42. Lammers, M.; Rose, R.; Scrima, A.; Wittinghofer, A. The regulation of mDia1 by autoinhibition and its release by Rho*GTP. *The EMBO journal* **2005**, *24*, 4176-4187, doi:10.1038/sj.emboj.7600879.
43. Rao, M.V.; Chu, P.H.; Hahn, K.M.; Zaidel-Bar, R. An optogenetic tool for the activation of endogenous diaphanous-related formins induces thickening of stress fibers without an increase in contractility. *Cytoskeleton (Hoboken, N.J.)* **2013**, *70*, 394-407, doi:10.1002/cm.21115.
44. Block, J.; Breitsprecher, D.; Kuhn, S.; Winterhoff, M.; Kage, F.; Geffers, R.; Duwe, P.; Rohn, J.L.; Baum, B.; Brakebusch, C., et al. FMNL2 drives actin-based protrusion and migration downstream of Cdc42. *Current biology : CB* **2012**, *22*, 1005-1012, doi:10.1016/j.cub.2012.03.064.
45. Blanchoin, L.; Michelot, A. Actin cytoskeleton: a team effort during actin assembly. *Current biology : CB* **2012**, *22*, R643-645, doi:10.1016/j.cub.2012.07.026.

46. Liu, B.; Dai, R.; Tian, C.J.; Dawson, L.; Gorelick, R.; Yu, X.F. Interaction of the human immunodeficiency virus type 1 nucleocapsid with actin. *Journal of virology* **1999**, *73*, 2901-2908.
47. Wilk, T.; Gowen, B.; Fuller, S.D. Actin associates with the nucleocapsid domain of the human immunodeficiency virus Gag polyprotein. *Journal of virology* **1999**, *73*, 1931-1940.
48. Zhao, H.; Datta, S.A.K.; Kim, S.H.; To, S.C.; Chaturvedi, S.K.; Rein, A.; Schuck, P. Nucleic acid-induced dimerization of HIV-1 Gag protein. *The Journal of biological chemistry* **2019**, *294*, 16480-16493, doi:10.1074/jbc.RA119.010580.
49. Crist, R.M.; Datta, S.A.; Stephen, A.G.; Soheilian, F.; Mirro, J.; Fisher, R.J.; Nagashima, K.; Rein, A. Assembly properties of human immunodeficiency virus type 1 Gag-leucine zipper chimeras: implications for retrovirus assembly. *Journal of virology* **2009**, *83*, 2216-2225, doi:10.1128/jvi.02031-08.
50. von Schwedler, U.K.; Stray, K.M.; Garrus, J.E.; Sundquist, W.I. Functional surfaces of the human immunodeficiency virus type 1 capsid protein. *Journal of virology* **2003**, *77*, 5439-5450, doi:10.1128/jvi.77.9.5439-5450.2003.
51. Hogue, I.B.; Grover, J.R.; Soheilian, F.; Nagashima, K.; Ono, A. Gag induces the coalescence of clustered lipid rafts and tetraspanin-enriched microdomains at HIV-1 assembly sites on the plasma membrane. *Journal of virology* **2011**, *85*, 9749-9766, doi:10.1128/jvi.00743-11.
52. Ott, D.E.; Coren, L.V.; Johnson, D.G.; Kane, B.P.; Sowder, R.C., 2nd; Kim, Y.D.; Fisher, R.J.; Zhou, X.Z.; Lu, K.P.; Henderson, L.E. Actin-binding cellular proteins inside human immunodeficiency virus type 1. *Virology* **2000**, *266*, 42-51, doi:10.1006/viro.1999.0075.
53. Ott, D.E.; Coren, L.V.; Kane, B.P.; Busch, L.K.; Johnson, D.G.; Sowder, R.C., 2nd; Chertova, E.N.; Arthur, L.O.; Henderson, L.E. Cytoskeletal proteins inside human immunodeficiency virus type 1 virions. *Journal of virology* **1996**, *70*, 7734-7743.
54. Chertova, E.; Chertov, O.; Coren, L.V.; Roser, J.D.; Trubey, C.M.; Bess, J.W., Jr.; Sowder, R.C., 2nd; Barsov, E.; Hood, B.L.; Fisher, R.J., et al. Proteomic and biochemical analysis of purified human immunodeficiency virus type 1 produced from infected monocyte-derived macrophages. *Journal of virology* **2006**, *80*, 9039-9052, doi:10.1128/jvi.01013-06.
55. Linde, M.E.; Colquhoun, D.R.; Ubaida Mohien, C.; Kole, T.; Aquino, V.; Cotter, R.; Edwards, N.; Hildreth, J.E.; Graham, D.R. The conserved set of host proteins incorporated into HIV-1 virions suggests a common egress pathway in multiple cell types. *Journal of proteome research* **2013**, *12*, 2045-2054, doi:10.1021/pr300918r.
56. Stauffer, S.; Rahman, S.A.; de Marco, A.; Carlson, L.A.; Glass, B.; Oberwinkler, H.; Herold, N.; Briggs, J.A.; Muller, B.; Grunewald, K., et al. The nucleocapsid domain of Gag is dispensable for actin incorporation into HIV-1 and for association of viral budding sites with cortical F-actin. *Journal of virology* **2014**, *88*, 7893-7903, doi:10.1128/jvi.00428-14.
57. Delon, I.; Brown, N.H. Integrins and the actin cytoskeleton. *Current opinion in cell biology* **2007**, *19*, 43-50, doi:10.1016/j.ceb.2006.12.013.
58. Nelson, W.J.; Drees, F.; Yamada, S. Interaction of cadherin with the actin cytoskeleton. *Novartis Foundation symposium* **2005**, *269*, 159-168; discussion 168-177, 223-130.
59. Owen, D.; Campbell, L.J.; Littlefield, K.; Evetts, K.A.; Li, Z.; Sacks, D.B.; Lowe, P.N.; Mott, H.R. The IQGAP1-Rac1 and IQGAP1-Cdc42 interactions: interfaces differ between the complexes. *The Journal of biological chemistry* **2008**, *283*, 1692-1704, doi:10.1074/jbc.M707257200.

60. Fukata, M.; Nakagawa, M.; Itoh, N.; Kawajiri, A.; Yamaga, M.; Kuroda, S.; Kaibuchi, K. Involvement of IQGAP1, an effector of Rac1 and Cdc42 GTPases, in cell-cell dissociation during cell scattering. *Molecular and cellular biology* **2001**, *21*, 2165-2183, doi:10.1128/mcb.21.6.2165-2183.2001.
61. Brandt, D.T.; Grosse, R. Get to grips: steering local actin dynamics with IQGAPs. *EMBO reports* **2007**, *8*, 1019-1023, doi:10.1038/sj.embor.7401089.
62. Swart-Mataraza, J.M.; Li, Z.; Sacks, D.B. IQGAP1 is a component of Cdc42 signaling to the cytoskeleton. *The Journal of biological chemistry* **2002**, *277*, 24753-24763, doi:10.1074/jbc.M111165200.
63. Sugihara, K.; Nakatsuji, N.; Nakamura, K.; Nakao, K.; Hashimoto, R.; Otani, H.; Sakagami, H.; Kondo, H.; Nozawa, S.; Aiba, A., et al. Rac1 is required for the formation of three germ layers during gastrulation. *Oncogene* **1998**, *17*, 3427-3433, doi:10.1038/sj.onc.1202595.
64. Hart, T.; Chandrashekhar, M.; Aregger, M.; Steinhart, Z.; Brown, K.R.; MacLeod, G.; Mis, M.; Zimmermann, M.; Fradet-Turcotte, A.; Sun, S., et al. High-Resolution CRISPR Screens Reveal Fitness Genes and Genotype-Specific Cancer Liabilities. *Cell* **2015**, *163*, 1515-1526, doi:10.1016/j.cell.2015.11.015.
65. Chen, B.; Chou, H.T.; Brautigam, C.A.; Xing, W.; Yang, S.; Henry, L.; Doolittle, L.K.; Walz, T.; Rosen, M.K. Rac1 GTPase activates the WAVE regulatory complex through two distinct binding sites. *eLife* **2017**, *6*, doi:10.7554/eLife.29795.
66. Yan, C.; Martinez-Quiles, N.; Eden, S.; Shibata, T.; Takeshima, F.; Shinkura, R.; Fujiwara, Y.; Bronson, R.; Snapper, S.B.; Kirschner, M.W., et al. WAVE2 deficiency reveals distinct roles in embryogenesis and Rac-mediated actin-based motility. *The EMBO journal* **2003**, *22*, 3602-3612, doi:10.1093/emboj/cdg350.
67. Rahman, S.A.; Koch, P.; Weichsel, J.; Godinez, W.J.; Schwarz, U.; Rohr, K.; Lamb, D.C.; Krausslich, H.G.; Muller, B. Investigating the role of F-actin in human immunodeficiency virus assembly by live-cell microscopy. *Journal of virology* **2014**, *88*, 7904-7914, doi:10.1128/jvi.00431-14.
68. Daste, F.; Walrant, A.; Holst, M.R.; Gadsby, J.R.; Mason, J.; Lee, J.E.; Brook, D.; Mettlen, M.; Larsson, E.; Lee, S.F., et al. Control of actin polymerization via the coincidence of phosphoinositides and high membrane curvature. *The Journal of cell biology* **2017**, *216*, 3745-3765, doi:10.1083/jcb.201704061.
69. Gallop, J.L.; Walrant, A.; Cantley, L.C.; Kirschner, M.W. Phosphoinositides and membrane curvature switch the mode of actin polymerization via selective recruitment of toca-1 and Snx9. *Proceedings of the National Academy of Sciences of the United States of America* **2013**, *110*, 7193-7198, doi:10.1073/pnas.1305286110.
70. Sabo, Y.; de Los Santos, K.; Goff, S.P. IQGAP1 Negatively Regulates HIV-1 Gag Trafficking and Virion Production. *Cell Rep* **2020**, *30*, 4065-4081 e4064, doi:10.1016/j.celrep.2020.03.002.
71. Brandt, D.T.; Marion, S.; Griffiths, G.; Watanabe, T.; Kaibuchi, K.; Grosse, R. Dia1 and IQGAP1 interact in cell migration and phagocytic cup formation. *The Journal of cell biology* **2007**, *178*, 193-200, doi:10.1083/jcb.200612071.
72. Bensenor, L.B.; Kan, H.M.; Wang, N.; Wallrabe, H.; Davidson, L.A.; Cai, Y.; Schafer, D.A.; Bloom, G.S. IQGAP1 regulates cell motility by linking growth factor signaling to actin assembly. *Journal of cell science* **2007**, *120*, 658-669, doi:10.1242/jcs.03376.
73. Mehedi, M.; Collins, P.L.; Buchholz, U.J. A novel host factor for human respiratory syncytial virus. *Communicative & integrative biology* **2017**, *10*, e1319025, doi:10.1080/19420889.2017.1319025.
74. Mehedi, M.; McCarty, T.; Martin, S.E.; Le Nouen, C.; Buehler, E.; Chen, Y.C.; Smelkinson, M.; Ganesan, S.; Fischer, E.R.; Brock, L.G., et al. Actin-Related Protein

2 (ARP2) and Virus-Induced Filopodia Facilitate Human Respiratory Syncytial Virus Spread. *PLoS pathogens* **2016**, *12*, e1006062, doi:10.1371/journal.ppat.1006062.

75. Martinez, M.G.; Kielian, M. Intercellular Extensions Are Induced by the Alphavirus Structural Proteins and Mediate Virus Transmission. *PLoS pathogens* **2016**, *12*, e1006061, doi:10.1371/journal.ppat.1006061.
76. Sherer, N.M.; Lehmann, M.J.; Jimenez-Soto, L.F.; Horensavitz, C.; Pypaert, M.; Mothes, W. Retroviruses can establish filopodial bridges for efficient cell-to-cell transmission. *Nature cell biology* **2007**, *9*, 310-315, doi:10.1038/ncb1544.
77. Cifuentes-Munoz, N.; Dutch, R.E.; Cattaneo, R. Direct cell-to-cell transmission of respiratory viruses: The fast lanes. *PLoS pathogens* **2018**, *14*, e1007015, doi:10.1371/journal.ppat.1007015.
78. Fukata, M.; Kuroda, S.; Fujii, K.; Nakamura, T.; Shoji, I.; Matsuura, Y.; Okawa, K.; Iwamatsu, A.; Kikuchi, A.; Kaibuchi, K. Regulation of cross-linking of actin filament by IQGAP1, a target for Cdc42. *The Journal of biological chemistry* **1997**, *272*, 29579-29583, doi:10.1074/jbc.272.47.29579.
79. Bendjennat, M.; Saffarian, S. The Race against Protease Activation Defines the Role of ESCRTs in HIV Budding. *PLoS pathogens* **2016**, *12*, e1005657, doi:10.1371/journal.ppat.1005657.
80. Ziv, N.E.; Smith, S.J. Evidence for a role of dendritic filopodia in synaptogenesis and spine formation. *Neuron* **1996**, *17*, 91-102, doi:10.1016/s0896-6273(00)80283-4.
81. Niell, C.M.; Meyer, M.P.; Smith, S.J. In vivo imaging of synapse formation on a growing dendritic arbor. *Nature neuroscience* **2004**, *7*, 254-260, doi:10.1038/nn1191.
82. Vasioukhin, V.; Bauer, C.; Yin, M.; Fuchs, E. Directed actin polymerization is the driving force for epithelial cell-cell adhesion. *Cell* **2000**, *100*, 209-219, doi:10.1016/s0092-8674(00)81559-7.
83. Menna, E.; Fossati, G.; Scita, G.; Matteoli, M. From filopodia to synapses: the role of actin-capping and anti-capping proteins. *The European journal of neuroscience* **2011**, *34*, 1655-1662, doi:10.1111/j.1460-9568.2011.07897.x.
84. Mothes, W.; Sherer, N.M.; Jin, J.; Zhong, P. Virus cell-to-cell transmission. *Journal of virology* **2010**, *84*, 8360-8368, doi:10.1128/jvi.00443-10.
85. Izumi, G.; Sakisaka, T.; Baba, T.; Tanaka, S.; Morimoto, K.; Takai, Y. Endocytosis of E-cadherin regulated by Rac and Cdc42 small G proteins through IQGAP1 and actin filaments. *The Journal of cell biology* **2004**, *166*, 237-248, doi:10.1083/jcb.200401078.
86. Kuroda, S.; Fukata, M.; Nakagawa, M.; Kaibuchi, K. Cdc42, Rac1, and their effector IQGAP1 as molecular switches for cadherin-mediated cell-cell adhesion. *Biochem Biophys Res Commun* **1999**, *262*, 1-6, doi:10.1006/bbrc.1999.1122.
87. Morita, E.; Sandrin, V.; Chung, H.Y.; Morham, S.G.; Gygi, S.P.; Rodesch, C.K.; Sundquist, W.I. Human ESCRT and ALIX proteins interact with proteins of the midbody and function in cytokinesis. *The EMBO journal* **2007**, *26*, 4215-4227, doi:10.1038/sj.emboj.7601850.
88. Le Clainche, C.; Schlaepfer, D.; Ferrari, A.; Klingauf, M.; Grohmanova, K.; Veligodskiy, A.; Didry, D.; Le, D.; Egile, C.; Carlier, M.F., et al. IQGAP1 stimulates actin assembly through the N-WASP-Arp2/3 pathway. *The Journal of biological chemistry* **2007**, *282*, 426-435, doi:10.1074/jbc.M607711200.
89. Choudhuri, K.; Llodra, J.; Roth, E.W.; Tsai, J.; Gordo, S.; Wucherpfennig, K.W.; Kam, L.C.; Stokes, D.L.; Dustin, M.L. Polarized release of T-cell-receptor-enriched microvesicles at the immunological synapse. *Nature* **2014**, *507*, 118-123, doi:10.1038/nature12951.
90. Chemin, K.; Bohineust, A.; Dogniaux, S.; Tourret, M.; Guegan, S.; Miro, F.; Hivroz, C. Cytokine secretion by CD4+ T cells at the immunological synapse requires Cdc42-

dependent local actin remodeling but not microtubule organizing center polarity. *Journal of immunology (Baltimore, Md. : 1950)* **2012**, *189*, 2159-2168, doi:10.4049/jimmunol.1200156.

91. Stinchcombe, J.C.; Majorovits, E.; Bossi, G.; Fuller, S.; Griffiths, G.M. Centrosome polarization delivers secretory granules to the immunological synapse. *Nature* **2006**, *443*, 462-465, doi:10.1038/nature05071.
92. Vardhana, S.; Choudhuri, K.; Varma, R.; Dustin, M.L. Essential role of ubiquitin and TSG101 protein in formation and function of the central supramolecular activation cluster. *Immunity* **2010**, *32*, 531-540, doi:10.1016/j.immuni.2010.04.005.
93. Rittmeyer, E.N.; Daniel, S.; Hsu, S.C.; Osman, M.A. A dual role for IQGAP1 in regulating exocytosis. *Journal of cell science* **2008**, *121*, 391-403, doi:10.1242/jcs.016881.
94. Damsky, C.H.; Sheffield, J.B.; Tuszynski, G.P.; Warren, L. Is there a role for actin in virus budding? *The Journal of cell biology* **1977**, *75*, 593-605, doi:10.1083/jcb.75.2.593.
95. Jouvenet, N.; Windsor, M.; Rietdorf, J.; Hawes, P.; Monaghan, P.; Way, M.; Wileman, T. African swine fever virus induces filopodia-like projections at the plasma membrane. *Cellular microbiology* **2006**, *8*, 1803-1811, doi:10.1111/j.1462-5822.2006.00750.x.
96. Kolesnikova, L.; Bohil, A.B.; Cheney, R.E.; Becker, S. Budding of Marburgvirus is associated with filopodia. *Cellular microbiology* **2007**, *9*, 939-951, doi:10.1111/j.1462-5822.2006.00842.x.
97. Kolesnikova, L.; Heck, S.; Matrosovich, T.; Klenk, H.D.; Becker, S.; Matrosovich, M. Influenza virus budding from the tips of cellular microvilli in differentiated human airway epithelial cells. *The Journal of general virology* **2013**, *94*, 971-976, doi:10.1099/vir.0.049239-0.
98. Carpenter, J.E.; Hutchinson, J.A.; Jackson, W.; Grose, C. Egress of light particles among filopodia on the surface of Varicella-Zoster virus-infected cells. *Journal of virology* **2008**, *82*, 2821-2835, doi:10.1128/jvi.01821-07.
99. Chang, K.; Baginski, J.; Hassan, S.F.; Volin, M.; Shukla, D.; Tiwari, V. Filopodia and Viruses: An Analysis of Membrane Processes in Entry Mechanisms. *Frontiers in microbiology* **2016**, *7*, 300, doi:10.3389/fmicb.2016.00300.
100. Lemichez, E.; Aktories, K. Hijacking of Rho GTPases during bacterial infection. *Experimental cell research* **2013**, *319*, 2329-2336, doi:10.1016/j.yexcr.2013.04.021.
101. Van den Broeke, C.; Jacob, T.; Favoreel, H.W. Rho'ing in and out of cells: viral interactions with Rho GTPase signaling. *Small GTPases* **2014**, *5*, e28318, doi:10.4161/sgtp.28318.
102. Gouin, E.; Welch, M.D.; Cossart, P. Actin-based motility of intracellular pathogens. *Current opinion in microbiology* **2005**, *8*, 35-45, doi:10.1016/j.mib.2004.12.013.
103. Small, J.V. Pushing with actin: from cells to pathogens. *Biochemical Society transactions* **2015**, *43*, 84-91, doi:10.1042/bst20140184.
104. Welch, M.D.; Way, M. Arp2/3-mediated actin-based motility: a tail of pathogen abuse. *Cell host & microbe* **2013**, *14*, 242-255, doi:10.1016/j.chom.2013.08.011.
105. Kim, H.; White, C.D.; Sacks, D.B. IQGAP1 in microbial pathogenesis: Targeting the actin cytoskeleton. *FEBS letters* **2011**, *585*, 723-729, doi:10.1016/j.febslet.2011.01.041.
106. Leung, J.; Yueh, A.; Appah, F.S., Jr.; Yuan, B.; de los Santos, K.; Goff, S.P. Interaction of Moloney murine leukemia virus matrix protein with IQGAP. *The EMBO journal* **2006**, *25*, 2155-2166, doi:10.1038/sj.emboj.7601097.
107. Gladue, D.P.; Holinka, L.G.; Fernandez-Sainz, I.J.; Prarat, M.V.; O'Donnell, V.; Vepkhvadze, N.G.; Lu, Z.; Risatti, G.R.; Borca, M.V. Interaction between Core protein

of classical swine fever virus with cellular IQGAP1 protein appears essential for virulence in swine. *Virology* **2011**, *412*, 68-74, doi:10.1016/j.virol.2010.12.060.

108. Dolnik, O.; Kolesnikova, L.; Welsch, S.; Strecker, T.; Schudt, G.; Becker, S. Interaction with Tsg101 is necessary for the efficient transport and release of nucleocapsids in marburg virus-infected cells. *PLoS pathogens* **2014**, *10*, e1004463, doi:10.1371/journal.ppat.1004463.

109. Dolnik, O.; Stevermann, L.; Kolesnikova, L.; Becker, S. Marburg virus inclusions: A virus-induced microcompartment and interface to multivesicular bodies and the late endosomal compartment. *European journal of cell biology* **2015**, *94*, 323-331, doi:10.1016/j.ejcb.2015.05.006.

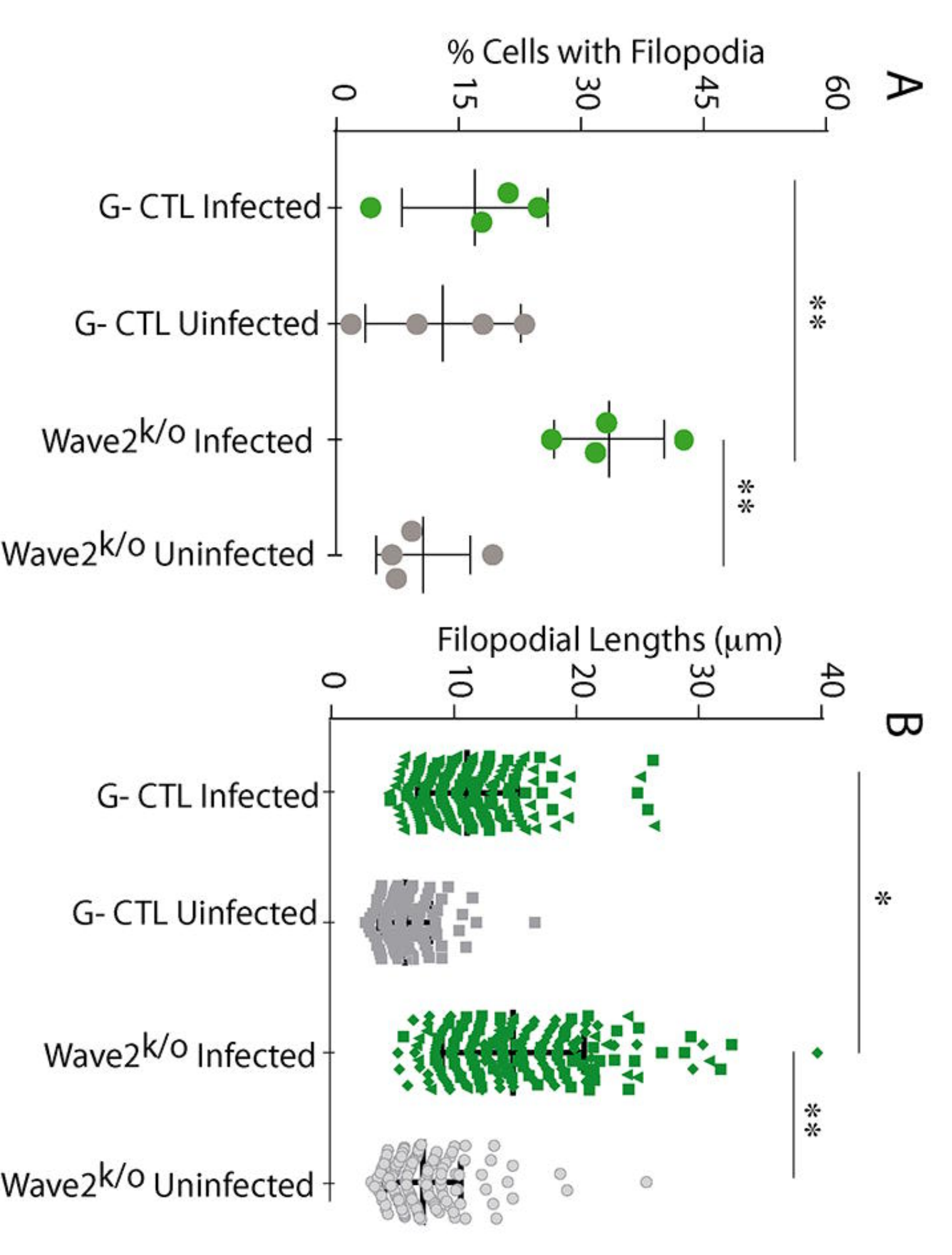
A
% Cells with Filopodia
0
15
30
45
60
G- CTL Infected
G- CTL Uinfected
Wave2k/o Infected
Wave2k/o Uninfected
**
**
B
Filopodial Lengths (µm)
0
10
20
30
40
G- CTL Infected
G- CTL Uinfected
Wave2k/o Infected
Wave2k/o Uninfected
*
**

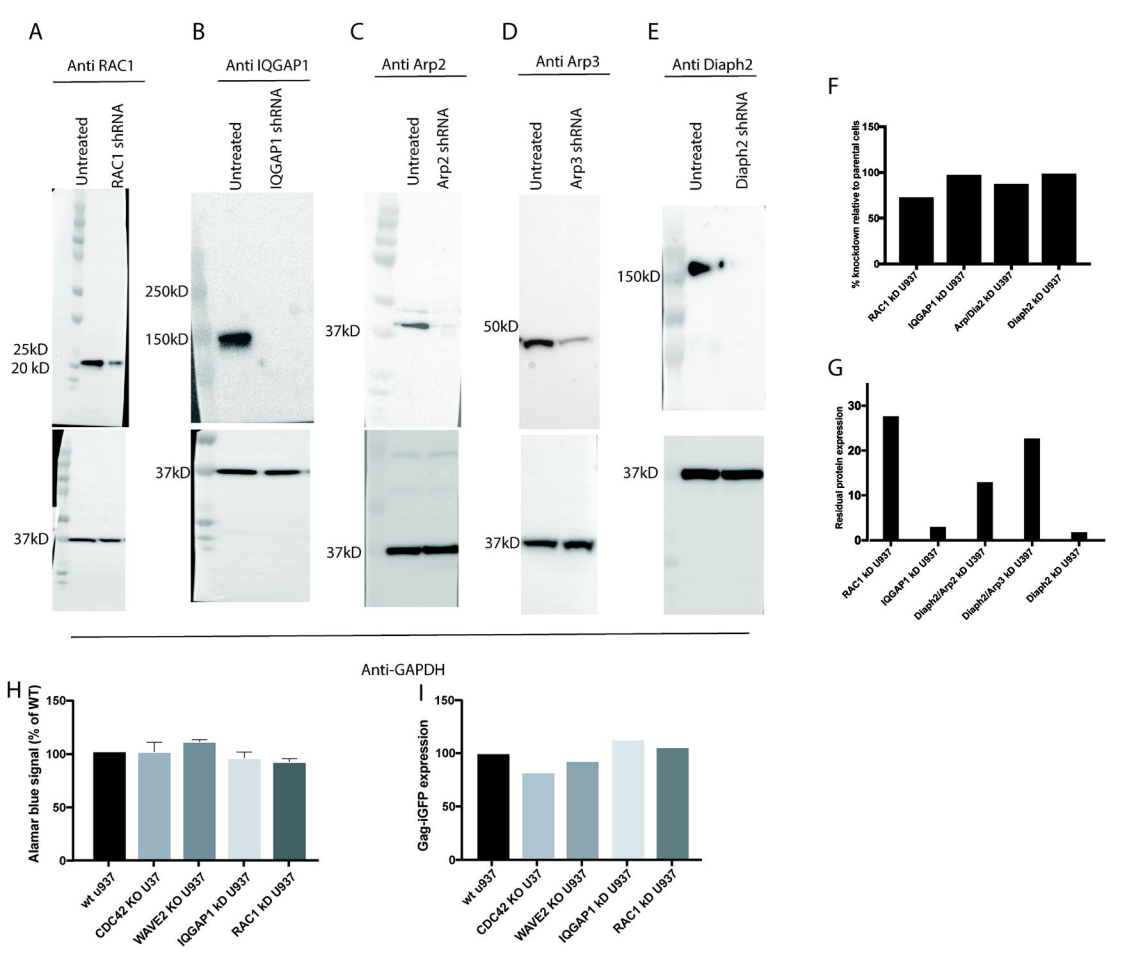
A
Anti RAC1
Untreated
RAC1 shRNA
25kD
20 kD
37kD
B
Anti IQGAP1
Untreated
IQGAP1 shRNA
250kD
150kD
37kD
C
Anti Arp2
Untreated
Arp2 shRNA
37kD
37kD
D
Anti Arp3
Untreated
Arp3 shRNA
50kD
37kD
E
Anti Diaph2
Untreated
Diaph2 shRNA
150kD
37kD
Anti-GAPDH
F
% knockdown relative to parental cells
150
100
50
0
RAC1 kD U937
IQGAP1 kD U937
Arp/Diaz kD U937
Diaph2 kD U937
G
Residual protein expression
30
20
10
0
RAC1 kD U937
IQGAP1 kD U937
Diaph2/Arp2 kD U937
Diaph2/Arp3 kD U937
Diaph2 kD U937
H
Alamar blue signal (% of WT)
150
100
50
0
wt u937
CDC42 KO U37
WAVE2 KO U937
IQGAP1 kD U937
RAC1 kD U937
I
Gag-iGFP expression
150
100
50
wt u937
CDC42 KO U37
WAVE2 KO U937
IQGAP1 kD U937
RAC1 kD U937

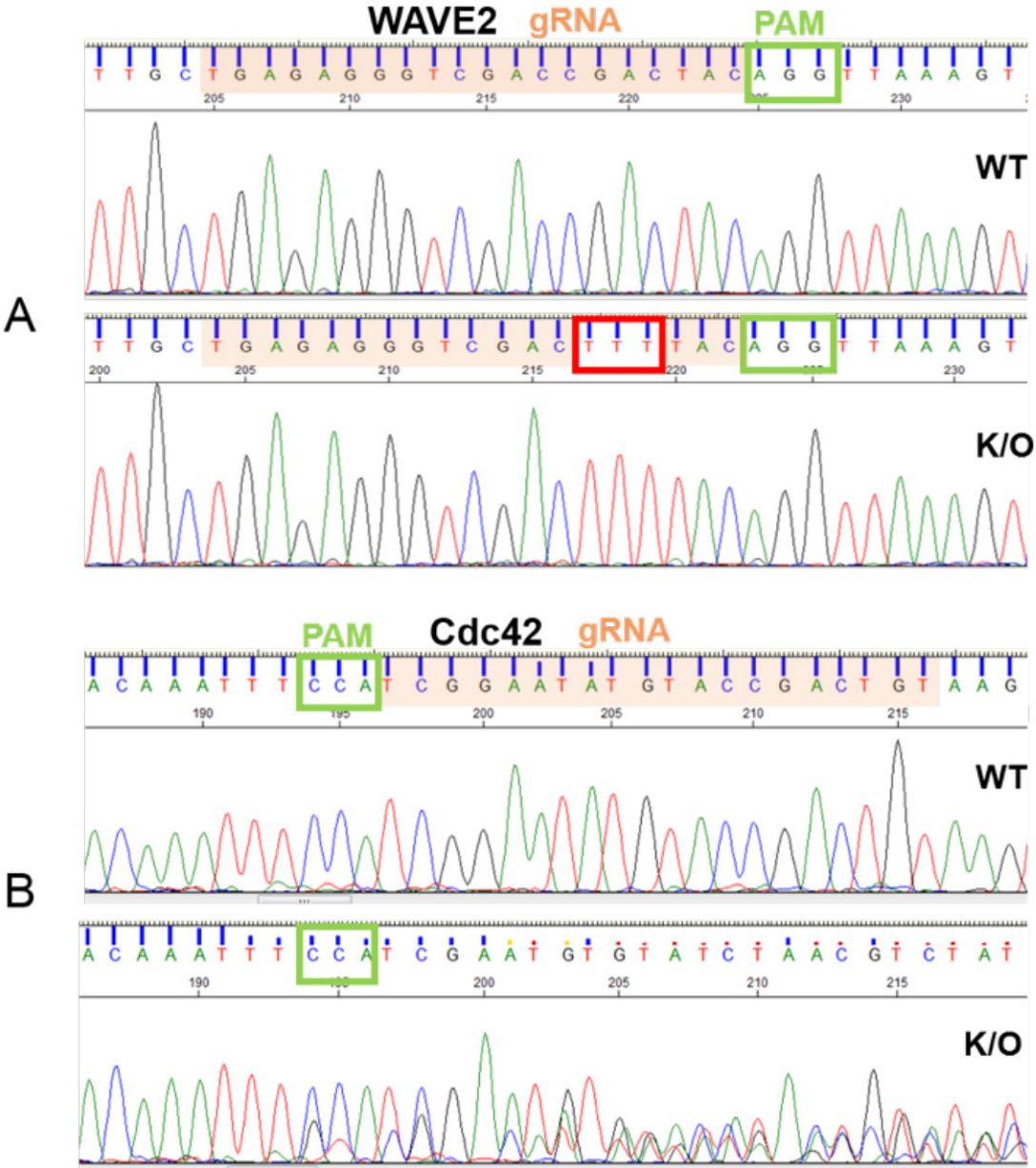
WAVE2
gRNA
PAM
WT
K/O
A
Cdc42
PAM
gRNA
WT
K/O
B

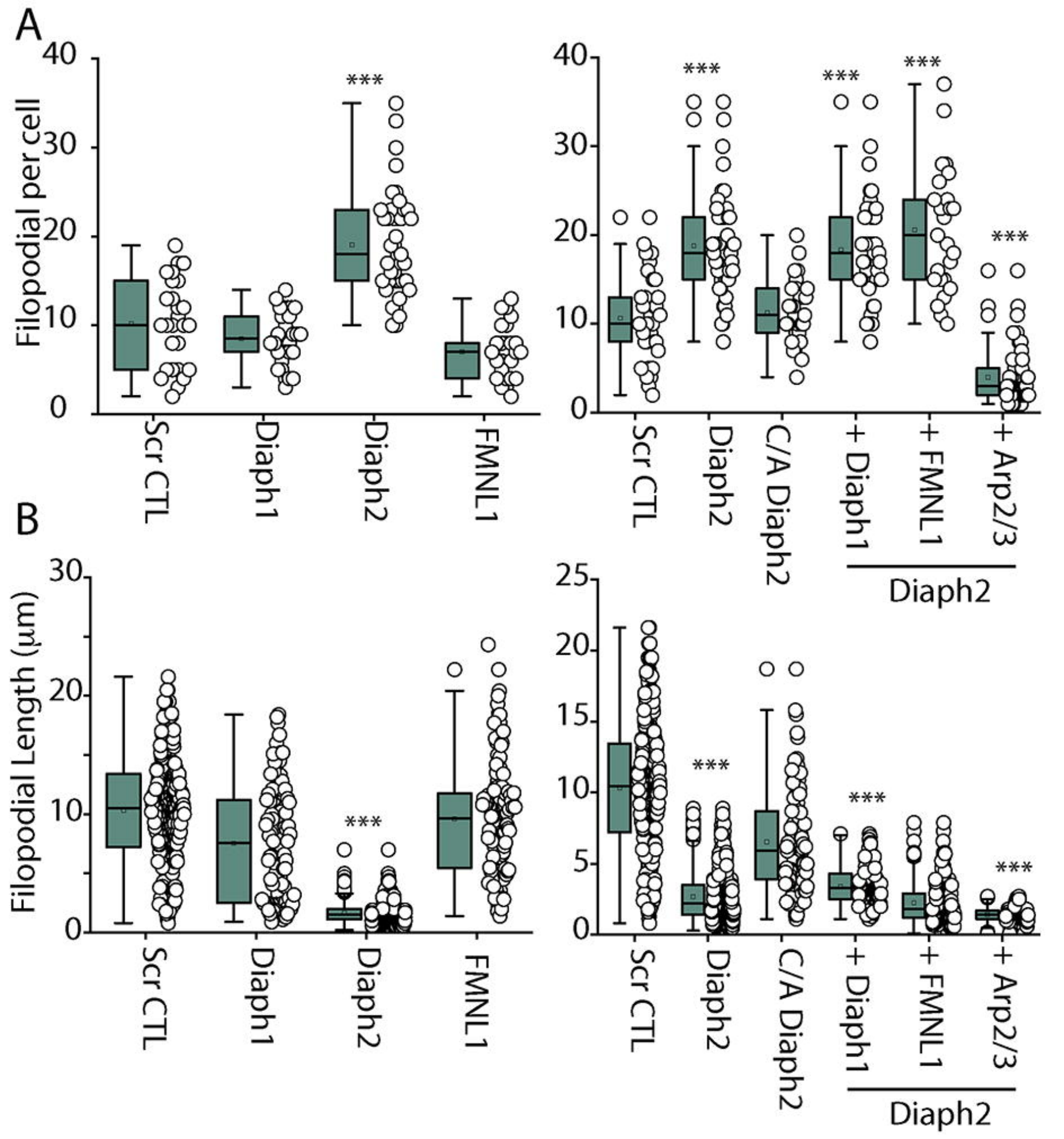
A
Filopodial per cell
0
10
20
30
40
***
Scr CTL
Diaph1
Diaph2
FMNL1
Scr CTL
Diaph2
C/A Diaph2
+ Diaph1
+ FMNL1
+ Arp2/3
Diaph2
B
Filopodial Length (µm)
0
5
10
15
20
25
30
***
Scr CTL
Diaph1
Diaph2
FMNL1
Scr CTL
Diaph2
C/A Diaph2
+ Diaph1
+ FMNL1
+ Arp2/3
Diaph2

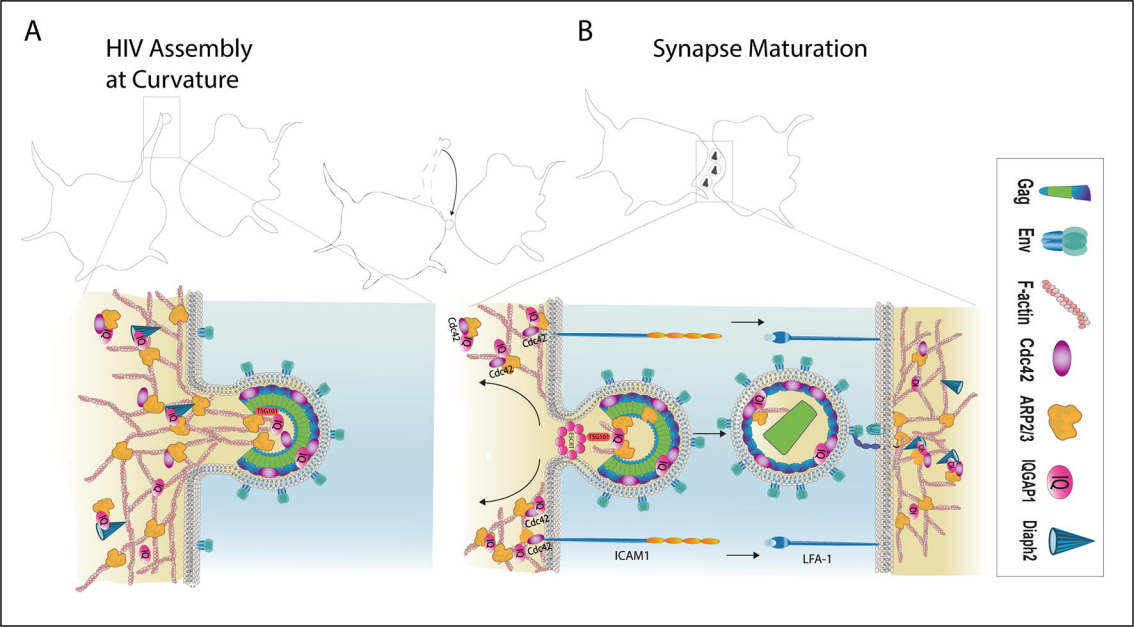
A
HIV Assembly
at Curvature
B
Synapse Maturation
Gag
Env
F-actin
Cdc42
ARP2/3
IQGAP1
Diaph2
IQ
TSG101
ICAM1
LFA-1

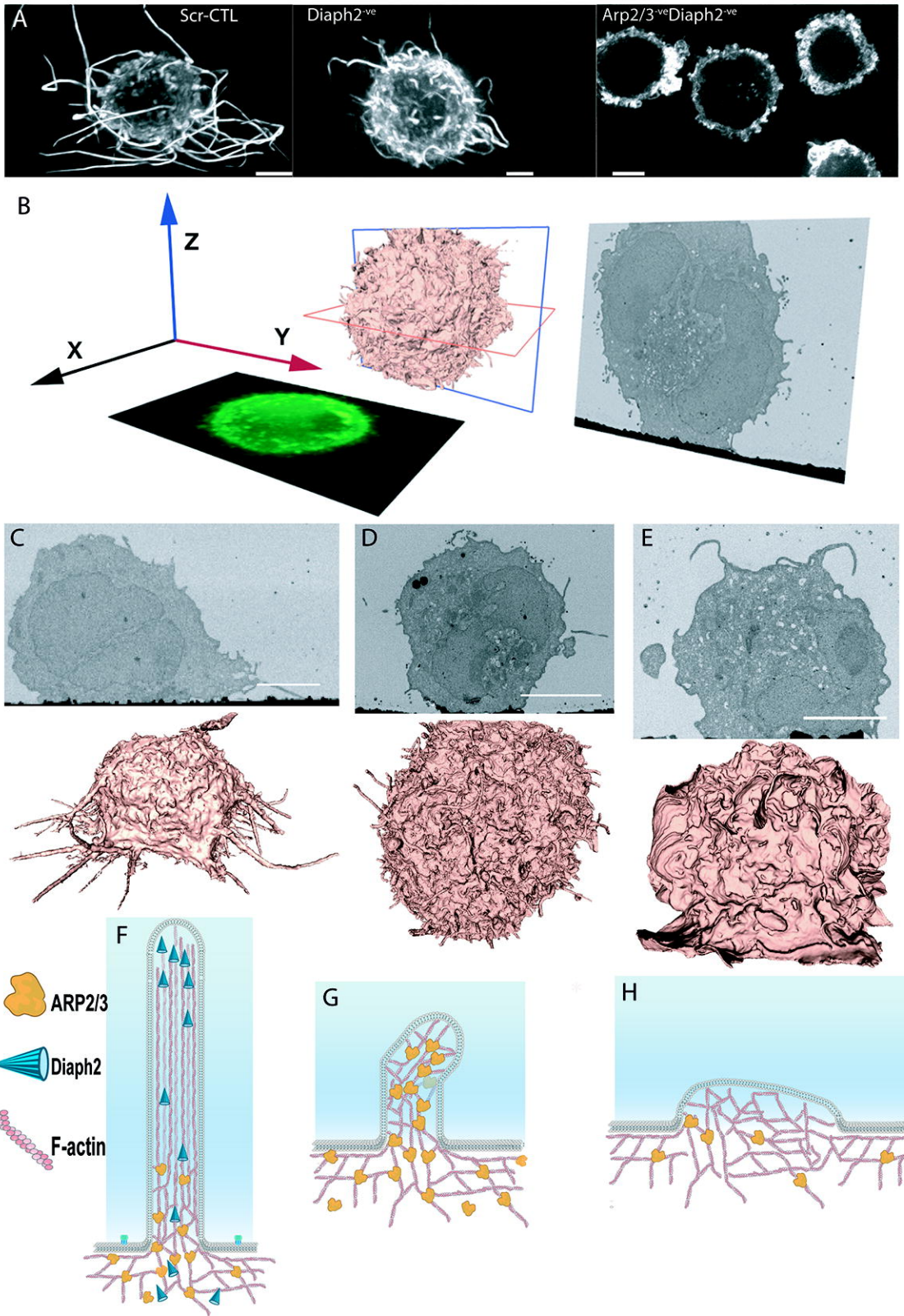
A
Scr-CTL
Diaph2-ve
Arp2/3-veDiaph2-ve
B
Z
X
Y
C
D
E
F
ARP2/3
Diaph2
F-actin
G
H

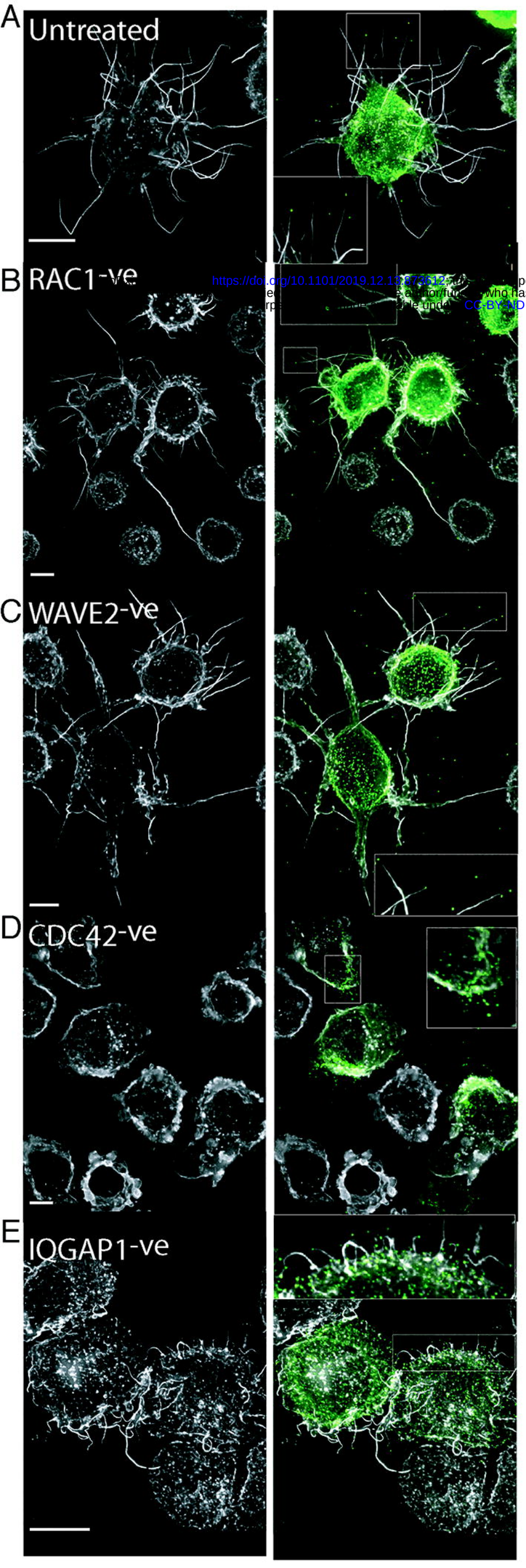

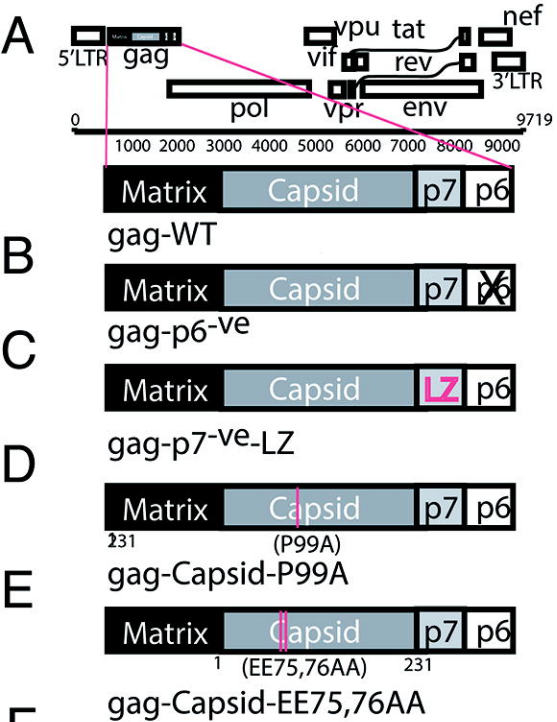
A
5'LTR
gag
vpu
tat
nef
vif
rev
3'LTR
pol
vpr
env
0
9719
1000 2000 3000 4000 5000 6000 7000 8000 9000
Matrix
Capsid
p7
p6
gag-WT
B
Matrix
Capsid
p7
p6
gag-p6-ve
C
Matrix
Capsid
LZ
p6
gag-p7-ve-LZ
D
Matrix
Capsid
p7
p6
231
(P99A)
gag-Capsid-P99A
E
Matrix
Capsid
p7
p6
1
(EE75,76AA)
231
gag-Capsid-EE75,76AA

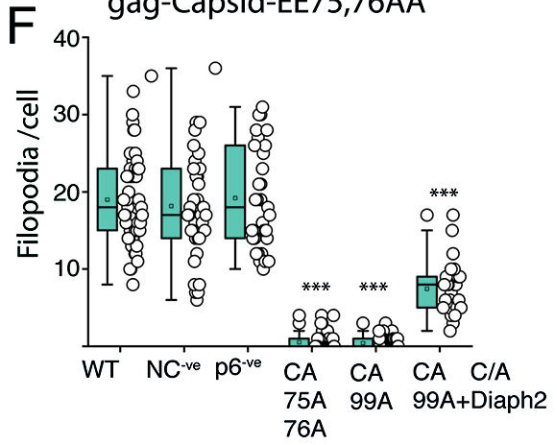
F
Filopodia /cell
40
30
20
10
***
***
***
WT
NC-ve
p6-ve
CA 75A 76A
CA 99A
CA 99A+Diaph2
C/A

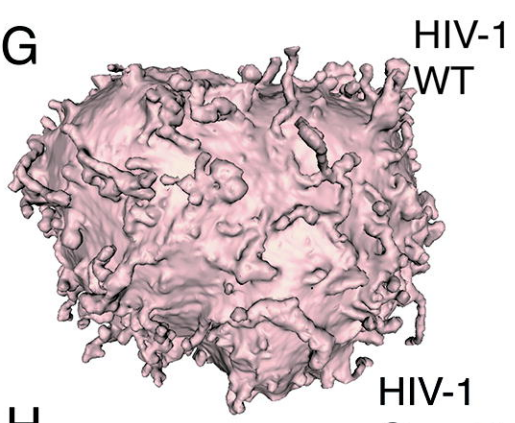
G
HIV-1 WT

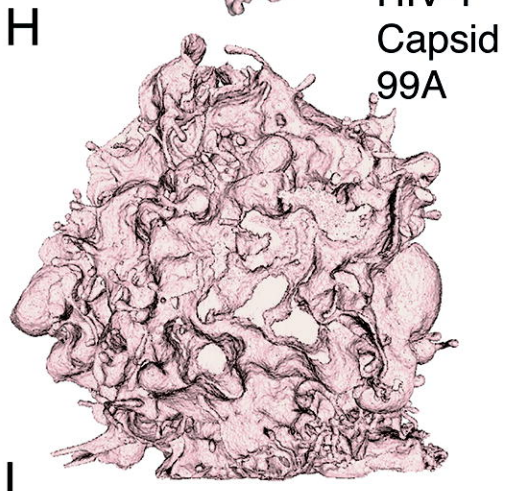
H
HIV-1 Capsid 99A

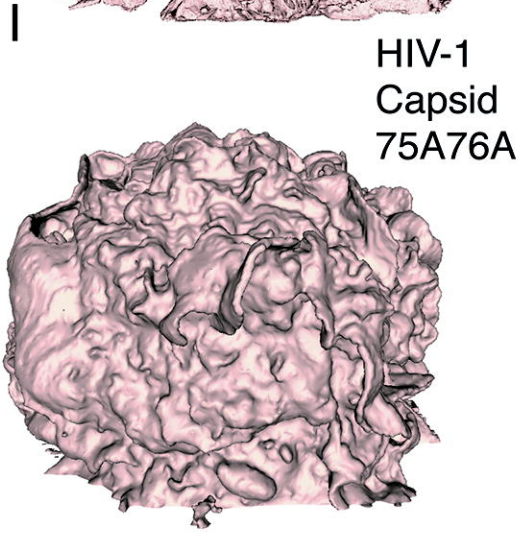
I
HIV-1 Capsid 75A76A

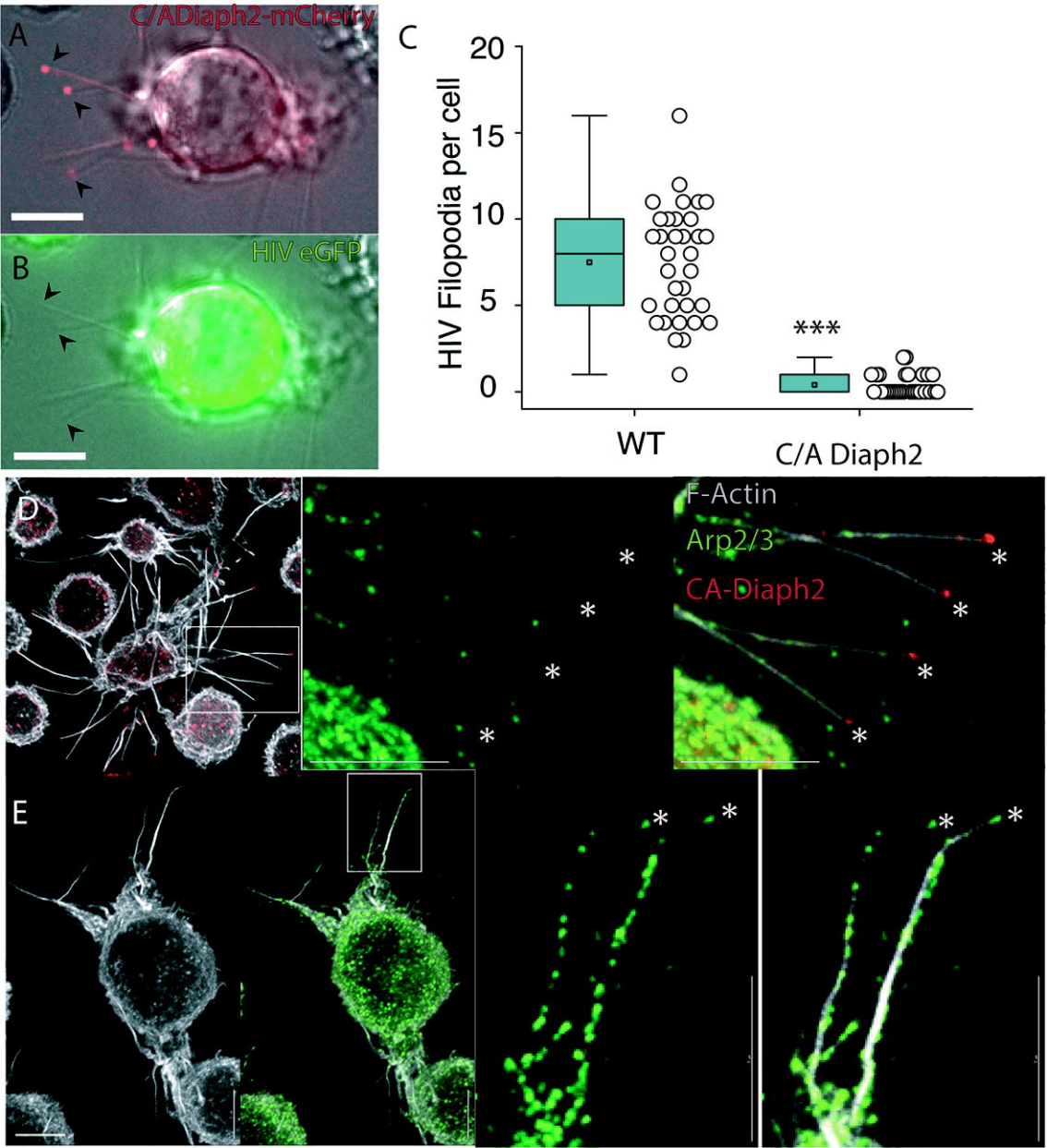
A
C/ADiaph2-mCherry
B
HIV eGFP
C
HIV Filopodia per cell
20
15
10
5
0
***
WT
C/A Diaph2
D
F-Actin
Arp2/3
CA-Diaph2
E

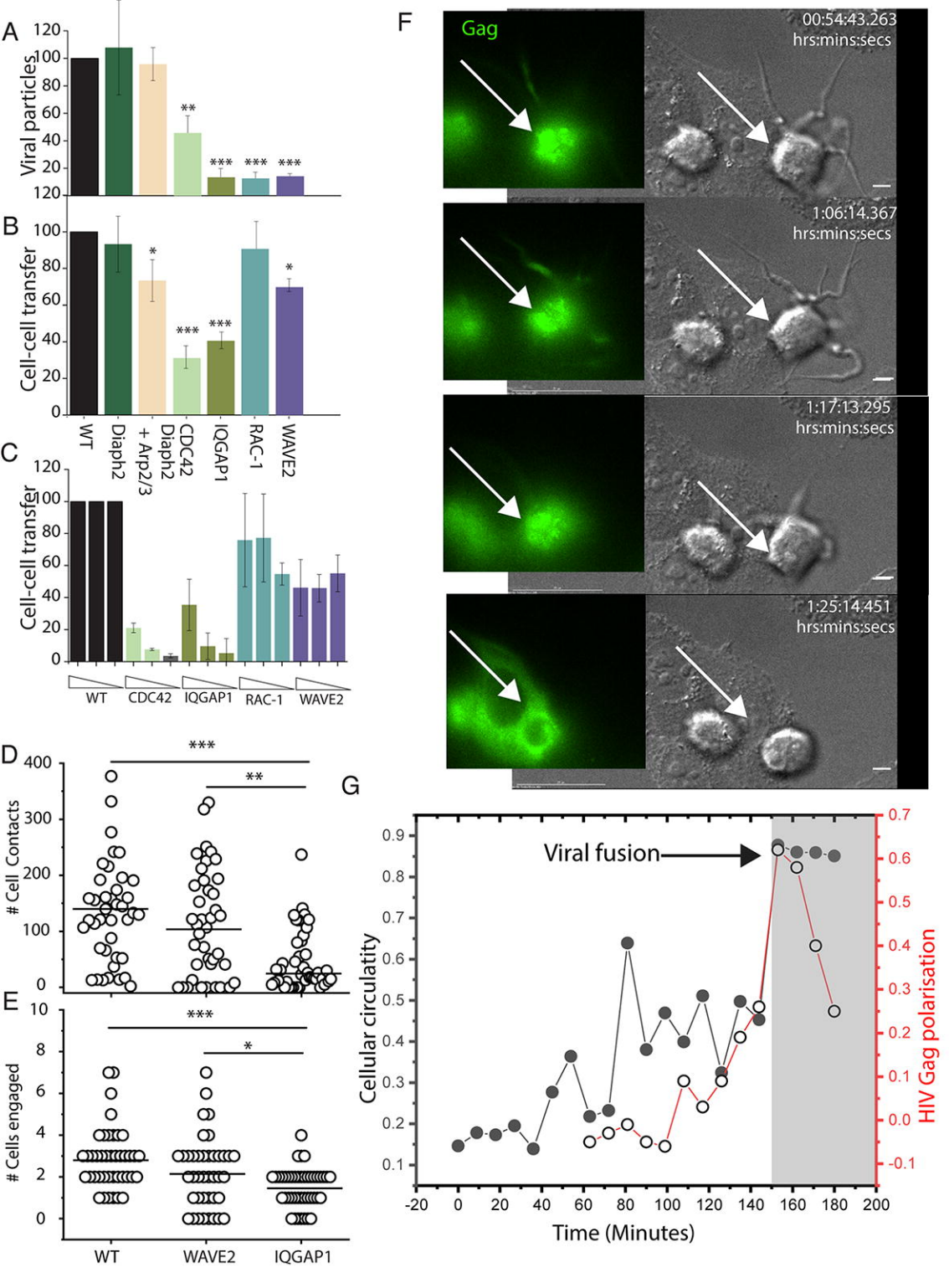
A
Viral particles
120
100
80
60
40
20
120
**
***
***
***
B
Cell-cell transfer
100
80
60
40
20
0
*
***
***
*
WT
Diaph2
+ Arp2/3
Diaph2
CDC42
IQGAP1
RAC-1
WAVE2
C
Cell-cell transfer
120
100
80
60
40
20
0
WT
CDC42
IQGAP1
RAC-1
WAVE2
D
Cell Contacts
400
300
200
100
0
***
**
E
Cells engaged
10
8
6
4
2
0
***
*
WT
WAVE2
IQGAP1
F
Gag
00:54:43.263
hrs:mins:secs
1:06:14.367
hrs:mins:secs
1:17:13.295
hrs:mins:secs
1:25:14.451
hrs:mins:secs
G
Viral fusion
Cellular circulatity
0.9
0.8
0.7
0.6
0.5
0.4
0.3
0.2
0.1
HIV Gag polarisation
0.7
0.6
0.5
0.4
0.3
0.2
0.1
0.0
-0.1
-20
0
20
40
60
80
100
120
140
160
180
200
Time (Minutes)

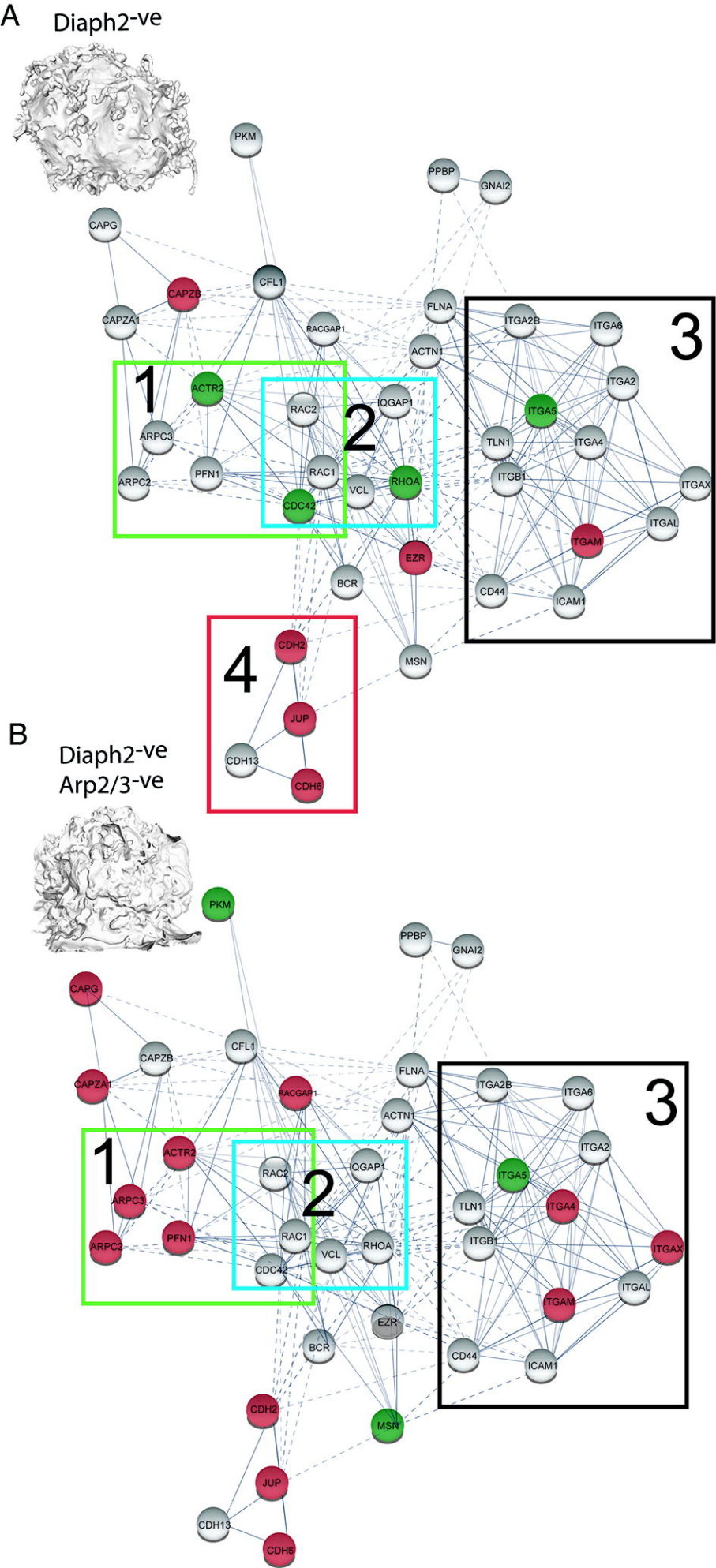
A
Diaph2-ve
PKM
PPBP
GNAI2
CAPG
CFL1
CAPZB
CAPZA1
FLNA
RACGAP1
ACTN1
ITGA2B
ITGA6
3
ITGA2
ACTR2
IQGAP1
RAC2
ITGA5
1
2
ARPC3
TLN1
ITGA4
PFN1
RAC1
ITGB1
ITGAX
ARPC2
VCL
RHOA
CDC42
ITGAL
ITGAM
EZR
BCR
CD44
ICAM1
4
CDH2
MSN
JUP
CDH13
CDH6
B
Diaph2-ve
Arp2/3-ve
PKM
PPBP
GNAI2
CAPG
CFL1
CAPZB
CAPZA1
FLNA
RACGAP1
ACTN1
ITGA2B
ITGA6
3
ITGA2
ITGA5
ACTR2
IQGAP1
RAC2
1
2
ARPC3
TLN1
ITGA4
PFN1
RAC1
ITGB1
ITGAX
ARPC2
VCL
RHOA
CDC42
ITGAL
ITGAM
EZR
BCR
CD44
ICAM1
CDH2
MSN
JUP
CDH13
CDH6